Pergamon

J. Quant. Spectrosc. Radiat. Transfer Vol. 57, No. 6, pp. 767–794, 1997
© 1997 Elsevier Science Ltd. All rights reserved
Printed in Great Britain
PII: S0022-4073(97)00012-5
0022-4073/97 $17.00 + 0.00

ASYMMETRY PARAMETERS OF THE PHASE FUNCTION FOR ISOLATED AND DENSELY PACKED SPHERICAL PARTICLES WITH MULTIPLE INTERNAL INCLUSIONS IN THE GEOMETRIC OPTICS LIMIT

M. I. MISHCHENKO and A. MÄCKE
NASA Goddard Institute for Space Studies, 2880 Broadway, New York, NY 10025, U.S.A.

(Received 2 August 1996)

Abstract—Since large, homogeneous dielectric particles have positive asymmetry parameters even when they are densely packed, it has been hypothesized that negative asymmetry parameters retrieved with Hapke's phenomenological model of bidirectional reflectance result from a complicated internal structure of planetary regolith particles. This paper tests that hypothesis by theoretically computing asymmetry parameters for isolated and densely packed composite spherical particles with size typical of regolith grains. It is assumed that the wavelength of the scattered light is much smaller than the particle size, and that particles are filled with large numbers of small inclusions. The computations show that it is essentially impossible to make asymmetry parameters of planetary regolith particles even slightly negative by filling the particles with large numbers of internal inclusions in the form of voids and/or grains with a refractive index substantially different from that of the host medium. Asymmetry parameters are positive even for densely packed composite particles with no internal absorption and extreme values of the internal scattering coefficient. Furthermore, they are sharply increased by even modest absorption inside composite particles, by reducing the refractive index contrast between the inclusions and the host particles, and/or by decreasing the packing density. Thus, the negative asymmetry parameters retrieved with Hapke's model need another explanation rather than assuming that they are real and are the result of a complicated internal structure of regolith particles. Besides the opposition-effect term, Hapke's model is nothing more than an approximate solution of the radiative transfer equation which inherently violates the energy conservation law. Therefore, the negative asymmetry parameters are likely to be numerical artefacts resulting from the approximations made in the model. © 1997 Elsevier Science Ltd

1. INTRODUCTION

By definition, a particle is called backscattering if the asymmetry parameter of the particle phase function is negative. Analogously, the particle is called forward-scattering if its asymmetry parameter is positive and is a neutral scatterer if the asymmetry parameter is equal to zero. The asymmetry parameter g is defined as[1]

$$g = \frac{1}{2}\int_{-1}^{1} \mathrm{d}(\cos\Theta)\cos\Theta p(\Theta)\,, \tag{1}$$

where Θ is the scattering angle (i.e., the angle between the incident and the scattered beams) and $p(\Theta)$ is the single-scattering phase function normalized according to the condition

$$\frac{1}{2}\int_{-1}^{1} \mathrm{d}(\cos\Theta)p(\Theta) = 1\,. \tag{2}$$

Theoretically, g can vary from -1 to $+1$. The extreme values correspond to backward and forward delta-function-like phase functions, respectively. The asymmetry parameter is an important scattering characteristic because, along with the single-scattering albedo, it controls the

radiative budget of an atmosphere or a scattering/absorbing layer and causes the presence or the absence of the atmospheric and solid-state greenhouse effects.[2-7]

In a recent paper (hereafter called Paper 1), Mishchenko[8] examined the effect of packing density on the asymmetry parameter of the single-scattering phase function for simple homogeneous particles.† In that analysis, he has used a theory which is based on solving Maxwell's equations to compute light scattering and on statistical mechanics to compute the statistics of mutual positions of densely packed particles.[9-11] Theoretical computations have shown that, even though the effect of packing density reduces the magnitude of the forward-scattering diffraction component of the phase function, it does not suppress it entirely (contrary to what is claimed in Ref. 12), especially for particles larger than a wavelength, and in most cases results in a minor reduction of the asymmetry parameter of the phase function. Most importantly, it has been demonstrated that the effect of packing density cannot make the asymmetry parameter negative if the ratio of the particle radius to the wavelength of light is larger than about 0.4. It should be emphasized that the theory used has a solid physical background and is in good quantitative agreement with results of controlled laboratory experiments.[13-16] Why controlled laboratory experiments, in contrast to what can be called laboratory observations, are so important in verifying the physical relevance of light scattering theories is discussed in the last section of Paper 1 (see also Refs. 17–19).

What is usually called the Hapke model of bidirectional reflectance[12, 20] is an approximate solution of the radiative transfer equation which is claimed to describe the scattering of light by particulate media with accuracy good enough for practical applications (whether or not the latter is true will be discussed in Sec. 4). It is well known that the model, when applied to the interpretation of bidirectional reflectance measurements of laboratory samples and terrestrial and planetary surfaces, systematically produces negative asymmetry parameters of the single-scattering phase function (e.g., Refs. 21–23 and references therein), thus contradicting the results of dense-medium asymmetry parameter calculations of Paper 1. Accurate radiative transfer computations reported in Paper 1 have demonstrated that those negative asymmetry parameters are unlikely to be real scattering characteristics of natural particles and are more probably a theoretical artefact resulting from an improper treatment of single- and multiple-scattering processes. In a recent publication[24] (hereafter called Paper 2), Hapke continues to claim that particles covering planetary surfaces are backscattering and suggests that they are backscattering because (1) their phase functions completely lack the diffraction component and (2) they contain cracks and voids and occur in the form of fragments of rocks and minerals welded together in optical contact. Therefore, the particles can be considered composite scatterers filled with multiple internal inclusions and, as a result, have negative asymmetry parameters.

Unfortunately, the conclusions of Paper 2 are based on qualitative speculations and, in part, on indirect laboratory observations rather than on accurate theoretical computations and true controlled laboratory experiments. Therefore, it is the primary goal of this paper to address the problem of the sign of the asymmetry parameter for composite particles with multiple internal inclusions by using state-of-the-art theoretical techniques. In Sec. 2, we use accurate Monte Carlo solutions of the radiative transfer equation subject to the Fresnel boundary condition to compute asymmetry parameters for large isolated particles with increasing numbers of internal inclusions. Both non-absorbing and absorbing cases are examined. In Sec. 3 we couple these isolated-particle calculations with the static structure factor theory[9-11] to compute asymmetry parameters for densely packed large particles with multiple internal inclusions. In Sec. 4, the implications of our results to remote sensing of planetary surfaces are discussed and the reliability and usefulness of the Hapke model are considered. Section 5 summarizes the main conclusions of this paper.

2. ISOLATED LARGE PARTICLES WITH INTERNAL INCLUSIONS

The asymmetry parameter can be quite easily computed for isolated homogeneous particles by using Mie theory for spheres,[1] the T-matrix approach[25, 26] for rotationally symmetric non-spherical

†We would like to draw the reader's attention to two typographical errors in Paper 1. Specifically, the first word of the fifth line of the second paragraph on p. 103 should read "larger", and the second line below Fig. 14 on p. 108 should read "...transfer equation had an asymmetry parameter $g = +0.82$, the retrieved model asymmetry..." Also, the second sentence on p. 97 should read as follows: "In general, this quantity depends on scattering angle and particle size distribution and shape."

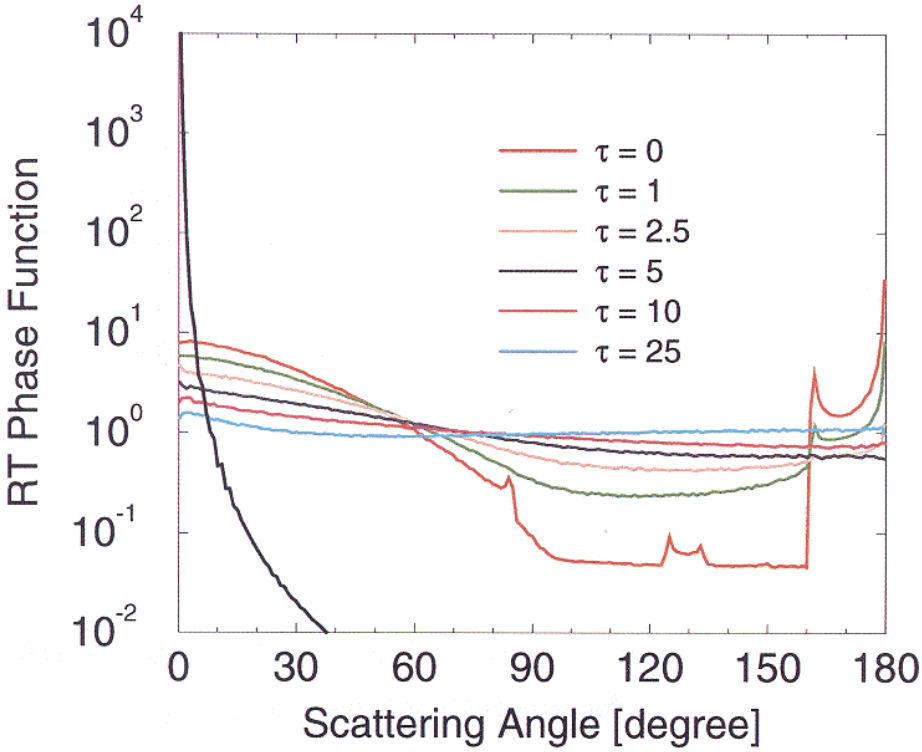

Plate 1. Ray-tracing phase function versus scattering angle for a 50 μm diameter composite particle with $m_{\mathrm{H}} = 1.55$, type 1 inclusions, and scattering optical thickness varying from 0 to 25. The internal single-scattering albedo, ω_{INT}, is equal to 1 (no absorption). The solid black curve shows the smoothed diffraction phase function.

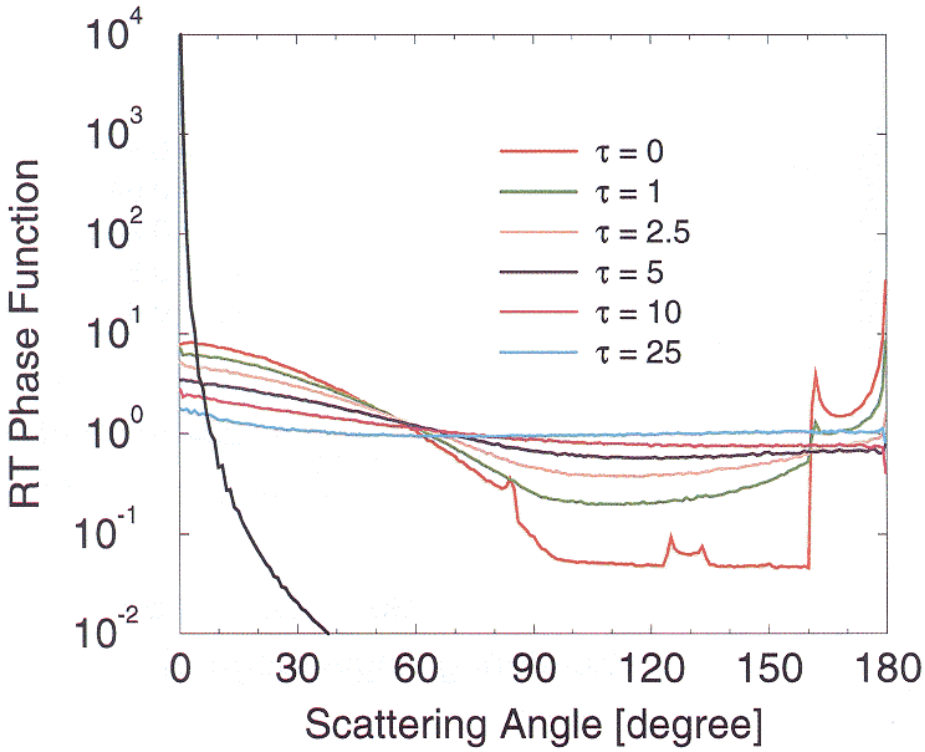

Plate 2. As in Plate 1, but for type 2 inclusions.

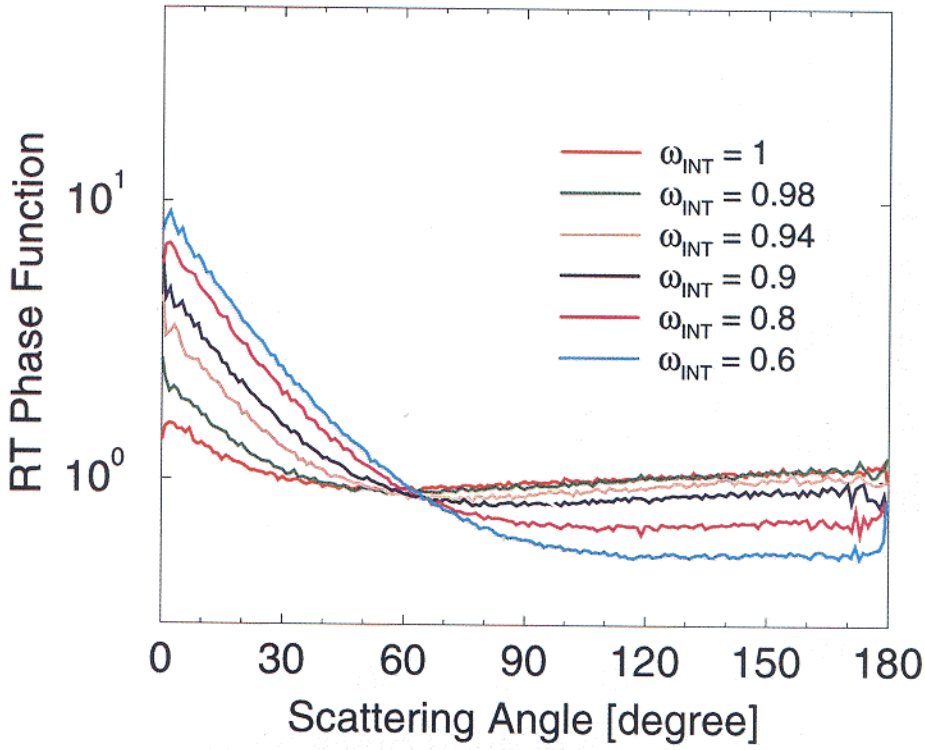

Plate 3. Ray-tracing phase function versus scattering angle for a 50 μm diameter composite particle with $m_H = 1.55$, type 1 inclusions, scattering optical thickness $\tau = 25$, and internal single-scattering albedo ω_{INT} varying from 1 to 0.6.

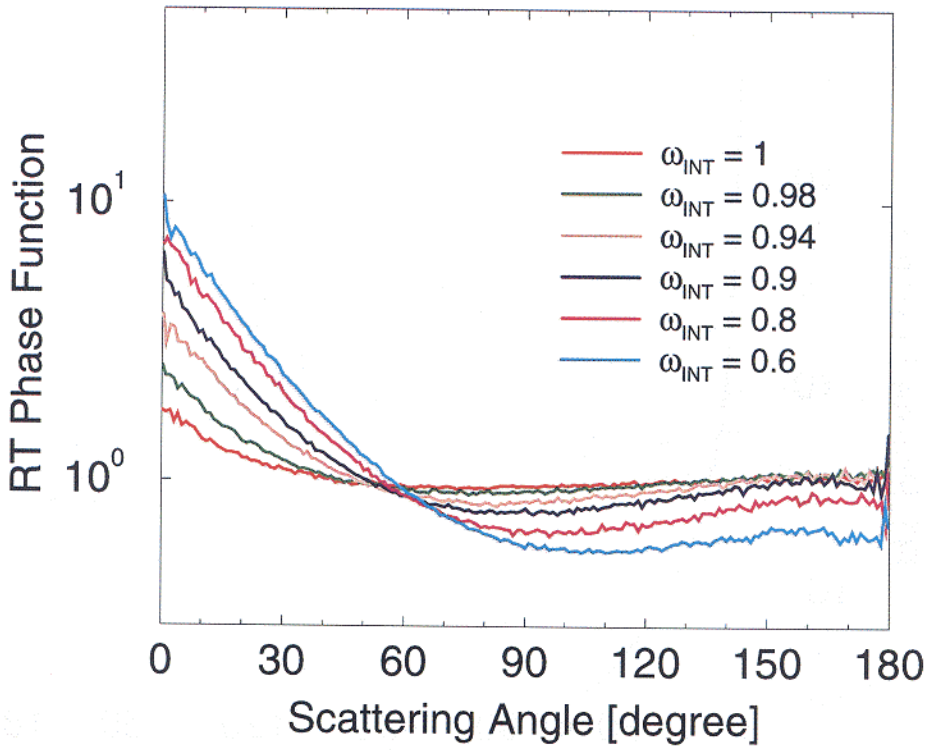

Plate 4. As in Plate 3, but for type 2 inclusions.

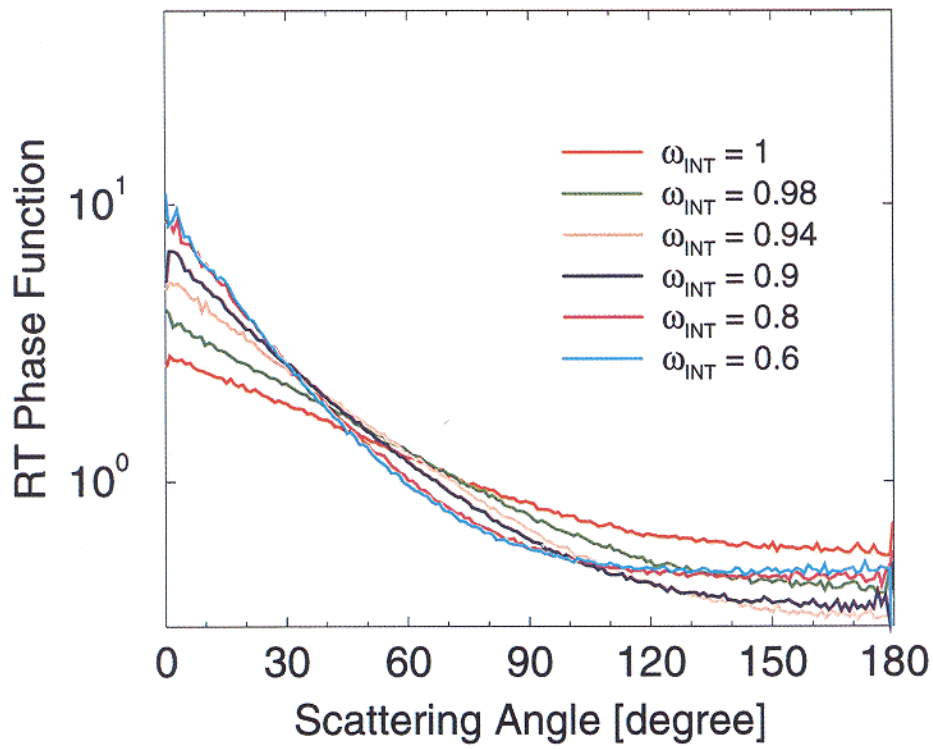

Plate 5. As in Plate 3, but for type 3 inclusions.

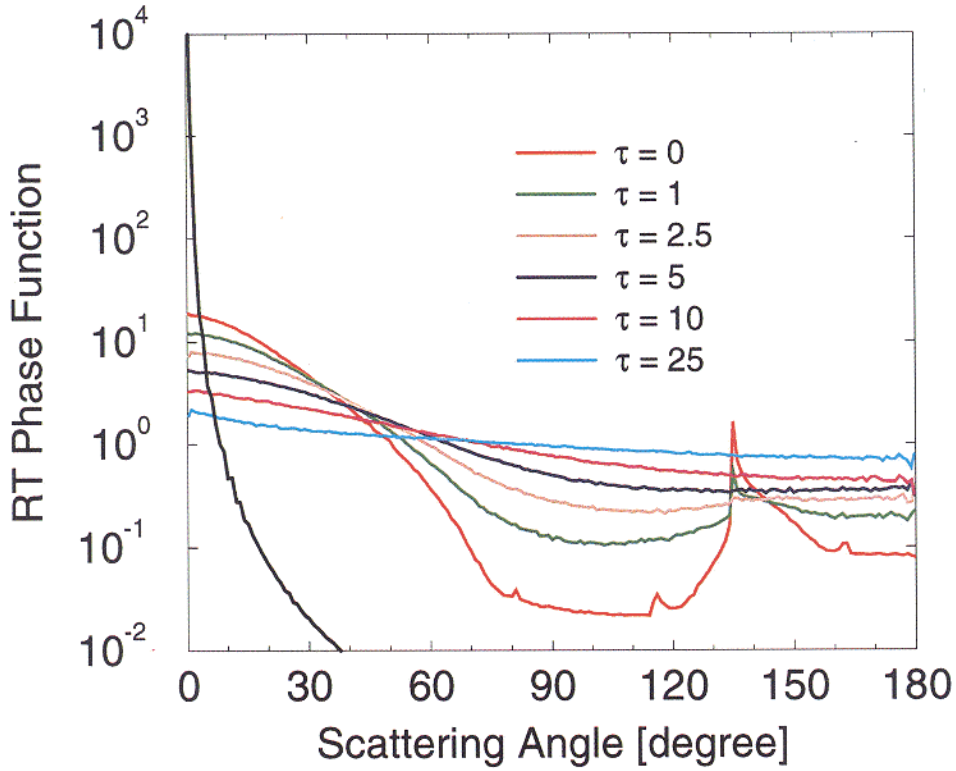

Plate 6. As in Plate 1, but for $m_H = 1.31$ and type 4 inclusions.

particles with equivalent-sphere size parameters less than about 130, and the geometric optics approximation[27–29] for non-spherical particles with larger size parameters.[26, 30] (The size parameter x of a spherical particle is defined as the ratio of the particle circumference to the wavelength of the incident light.) The calculation of the asymmetry parameter for an isolated particle with multiple internal inclusions is a more complicated problem. For composite particles with sizes smaller than or comparable to the wavelength, one can use the exact superposition T-matrix method[31–35] or the discrete dipole approximation (DDA).[36] However, regolith particles often have sizes much larger than the wavelength of the visible light, in which case the superposition T-matrix and DDA computations become excessively time consuming. Fortunately, in this case the use of the geometric optics approximation can be expected to provide a quite sufficient accuracy.[37, 38]

In our calculations, we assume that the composite particle is spherical with a diameter of $D = 50$ μm, thus corresponding to the average size of lunar soil grains,[39, 40] and the wavelength of the incident light is $\lambda = 0.55$ μm. The medium inside the particle is characterized by the host refractive index and by the refractive index, size distribution, and average number density of the inclusions. The host medium itself is assumed to be non-absorbing, whereas the inclusions can be either purely absorbing or purely scattering. The purely absorbing inclusions are submicrometre-sized grains of metallic iron, whereas the purely scattering inclusions are either voids (vacuum bubbles) or particles with a refractive index different from that of the host medium. We assume that the inclusions are wavelength-sized and, from the geometric optics standpoint, act as point-like objects with Mie phase functions. The refractive index of the host medium governs the processes of reflection and refraction of light beams by the particle surface via the Snell law and Fresnel's equations. The spatial distribution of the inclusions inside the composite particle is assumed to be totally random. Therefore, the interior of the particle as a whole is spherically symmetric, and multiple scattering of light inside the particle is described by the radiative transfer equation subject to the reflection/refraction boundary condition at the host particle surface.

The single-scattering properties of a small-volume element of the large-particle interior are specified by the internal single-scattering albedo, ω_{INT}, and the internal single-scattering phase function, $p_{\mathrm{INT}}(\Theta)$. Assuming for simplicity that the internal inclusions are spheres, the latter two quantities can be easily computed given the size distributions and number densities of the inclusions. Besides the Fresnel boundary condition, the only three parameters needed to solve the radiative transfer equation are the internal phase function and single-scattering albedo and the scattering optical thickness of the host particle; i.e., the product of the host particle diameter and the internal volume scattering coefficient. The latter quantity is equal to the product of the average scattering cross-section per inclusion and the average number density of the purely scattering inclusions.

The radiative transfer equation is solved using the Monte Carlo technique[37, 38] by tracing the history of 10^6 independent rays. We have found that this number of rays is quite sufficient to provide a high statistical accuracy of Monte Carlo computations even for non-absorbing particles. That this is indeed true is demonstrated by the weak statistical noise in the computed phase functions (see Plates 1 – 6). The output result of the Monte Carlo calculations is the ray-tracing single-scattering albedo, ω^{RT}, and the ray-tracing phase function, $P^{\mathrm{RT}}(\Theta)$, of the large composite particle. Since the ray-tracing extinction cross-section of the host particle is equal to its geometric cross-section S, $C_{\mathrm{ext}}^{\mathrm{RT}} = S = \pi D^2/4$, the ray-tracing scattering cross-section is equal to $C_{\mathrm{sca}}^{\mathrm{RT}} = \omega^{\mathrm{RT}} S$ and the ray-tracing absorption cross-section is given by $C_{\mathrm{abs}}^{\mathrm{RT}} = (1 - \omega^{\mathrm{RT}})S$. A more detailed description of the Monte Carlo ray-tracing method can be found in Ref. 37.

For a large isolated composite particle, the ray-tracing computations must be supplemented by the calculation of diffraction. The diffraction extinction cross-section is always equal to the diffraction scattering cross-section, $C_{\mathrm{ext}}^{\mathrm{D}} \equiv C_{\mathrm{sca}}^{\mathrm{D}}$, so that the diffraction single-scattering albedo is always equal to one: $\omega^{\mathrm{D}} \equiv 1$. Furthermore, for isolated particles the diffraction extinction cross-section is equal to the particle geometric cross-section, $C_{\mathrm{ext}}^{\mathrm{D}} = S$. For particles much larger than a wavelength, the diffraction phase function is given by the well-known formula[41]

$$\begin{cases} p^{\mathrm{D}}(\Theta) = 4x^2\left(\dfrac{J_1(x\sin\Theta)}{x\sin\Theta}\right)^2, & \Theta\in[0°,90°], \quad x\to\infty \\ p^{\mathrm{D}}(\Theta) = 0, & \Theta\in[90°,180°], \end{cases} \tag{3}$$

where $J_1(y)$ is the Bessel function of the first kind and $x = \pi D/\lambda$. Thus, the total optical cross-sections, single-scattering albedo, phase function, and asymmetry parameter for the large, isolated, composite particle are given by the following formulas:

$$C_{\mathrm{ext}} = C_{\mathrm{ext}}^{\mathrm{RT}} + C_{\mathrm{ext}}^{\mathrm{D}} = 2S\,, \tag{4}$$

$$C_{\mathrm{sca}} = C_{\mathrm{sca}}^{\mathrm{RT}} + C_{\mathrm{sca}}^{\mathrm{D}} = (1+\omega^{\mathrm{RT}})S\,, \tag{5}$$

$$\omega = \frac{C_{\mathrm{sca}}}{C_{\mathrm{ext}}} = \frac{\omega^{\mathrm{RT}}+1}{2}\,, \tag{6}$$

$$p(\Theta) = \frac{C_{\mathrm{sca}}^{\mathrm{RT}}p^{\mathrm{RT}}(\Theta) + C_{\mathrm{sca}}^{\mathrm{D}}p^{\mathrm{D}}(\Theta)}{C_{\mathrm{sca}}^{\mathrm{RT}} + C_{\mathrm{sca}}^{\mathrm{D}}} = \frac{\omega^{\mathrm{RT}}p^{\mathrm{RT}}(\Theta) + p^{\mathrm{D}}(\Theta)}{\omega^{\mathrm{RT}}+1}\,, \tag{7}$$

$$g = \frac{C_{\mathrm{sca}}^{\mathrm{RT}}g^{\mathrm{RT}} + C_{\mathrm{sca}}^{\mathrm{D}}g^{\mathrm{D}}}{C_{\mathrm{sca}}^{\mathrm{RT}} + C_{\mathrm{sca}}^{\mathrm{D}}} = \frac{\omega^{\mathrm{RT}}g^{\mathrm{RT}} + g^{\mathrm{D}}}{\omega^{\mathrm{RT}}+1}\,. \tag{8}$$

Note that for a sphere with $D = 50$ μm and a wavelength of $\lambda = 0.55$ μm, the diffraction asymmetry parameter g^{D} is equal to 0.99766..., i.e., its deviation from 1 is negligibly small.

The four types of internal inclusion used in this paper are summarized in Table 1 (note that all refractive indices are given relative to vacuum). Most of our calculations pertain to the refractive index of the host particle equal to $m_{\mathrm{H}} = 1.55$. This value is adopted as typical of silicate materials. For the purely scattering inclusions, two refractive indices are used. The first one, $m_1 = 1$, corresponds to voids inside the host particles (hereafter called type 1 inclusions), while the second one, $m_2 = 2$, corresponds to highly refractive grains (hereafter called type 2 inclusions). The inclusions are assumed to be distributed over radii r according to the standard gamma distribution[1]

$$n(r) = \text{const}\; r^{(1-3b)/b}\exp\left(-\frac{r}{ab}\right), \tag{9}$$

where $n(r)\,\mathrm{d}r$ is the fraction of inclusions with radii from r to $r + \mathrm{d}r$, a is the effective radius equal to 0.5 μm, b is the effective variance equal to 0.1, and the constant ensures the normalization

$$\int_0^\infty \mathrm{d}r\, n(r) = 1\,. \tag{10}$$

The single-scattering properties of the inclusions have been calculated by using the standard Mie theory. The scattering phase functions for both types of inclusion are shown in Fig. 1. Since both type 1 and type 2 inclusions are assumed to be non-absorbing, their single-scattering albedos are equal to 1. We do not explicitly model the absorbing inclusions in the form of submicrometre-sized grains of metal iron. Since these grains are assumed to be totally absorbing, they do not contribute to the volume scattering coefficient and scattering phase function of the large-particle interior. Their only effect is to reduce the internal single-scattering albedo, ω_{INT}. Therefore, we model the effect of increasing absorption inside the large composite particle by varying ω_{INT} from 1 to 0.

Plates 1 and 2 show the ray-tracing phase functions computed for 50 μm diameter host particles with type 1 and type 2 scattering inclusions, no absorbing inclusions, and scattering optical

Table 1. Four types of internal inclusion.

	Refractive index of the host medium	Refractive index of the inclusions
Type 1	1.55	1
Type 2	1.55	2
Type 3	1.55	1.65
Type 4	1.31	1

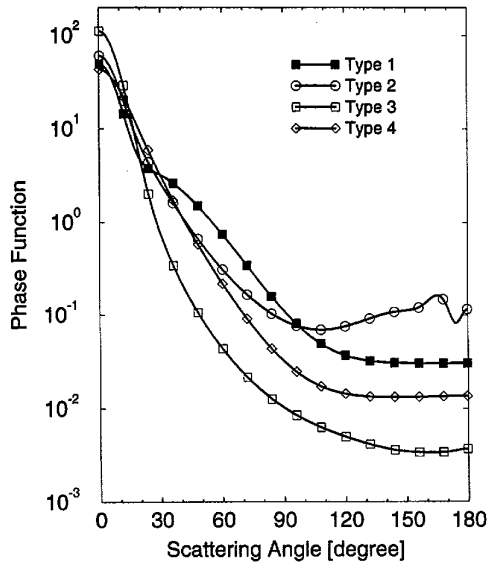

Fig. 1. Phase function versus scattering angle for four types of internal inclusion.

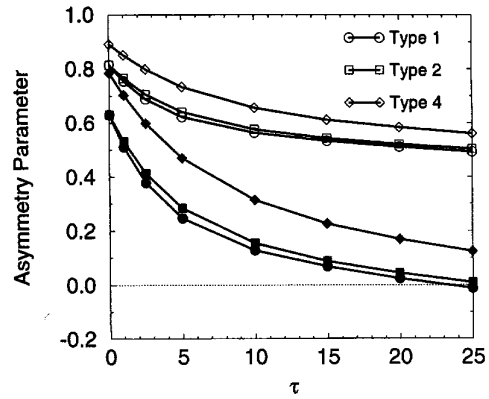

Fig. 2. Ray-tracing (filled symbols) and total (open symbols) asymmetry parameters versus scattering optical thickness for 50 μm diameter composite particles with type 1, type 2, and type 4 inclusions. The host refractive index is 1.55 for type 1 and type 2 inclusions and 1.31 for type 4 inclusions. The internal single-scattering albedo, ω_{INT}, is equal to 1 (no absorption).

thickness τ varying from 0 (no scattering inclusions) to 25. For comparison, the black curve shows the diffraction phase function smoothed by averaging over 1°-wide angular bins. It is seen that the ray-tracing phase function for the clear host particle (no inclusions) exhibits remarkable geometric optics features typical of large spherical particles and discussed in detail in Ref. 1. With increasing τ, these features rapidly vanish, and the ray-tracing phase functions become more and more isotropic, in qualitative agreement with laboratory measurements of Ref. 42. We did not perform computations for $\tau > 25$ since the scattering optical thickness $\tau = 25$ already seems to be an unrealistic extreme case. Indeed, the internal scattering coefficient for particles with $D = 50$ μm and $\tau = 25$ is so large that as short a path length inside the composite particle as 2 μm already attenuates a beam by a factor of $e \approx 2.72$ solely due to scattering. (Of course, internal absorption causes even further attenuation.) The internal scattering coefficient for the composite particle with $\tau = 25$ and $D = 50$ μm is as much as 23 times greater than that for the 1.26 cm diameter resin sphere measured in [42] and having what McGuire and Hapke call "a high density of internal scatterers", in contrast to two other measured resin spheres with a "low" and a "medium internal scattering density". Moreover, comparison of Plates 1 and 2 with phase functions measured for large, highly heterogeneous meteoritic particles[43] shows that the scattering optical thickness $\tau = 25$ already overstates the effect of internal structure on the scattering phase function. Note that for $\tau = 25$, the numbers of type 1 and type 2 inclusions inside a 50 μm diameter composite particle are 29,469 and 18,967 (!), respectively.

Equation (8) with $g^{\mathrm{D}} = 0.99766\ldots$ unequivocally suggests that the total asymmetry parameter for a large, isolated, composite particle cannot be negative. Furthermore, the only way to obtain the total asymmetry parameter equal to zero is to have only non-absorbing inclusions and a backward delta-function-like ray-tracing phase function so that $\omega^{\mathrm{RT}} = 1$ and $g^{\mathrm{RT}} = -1$. Figure 2 shows that with increasing scattering optical thickness τ, the ray-tracing asymmetry parameter g^{RT} for the 50 μm diameter composite particle with no absorption decreases systematically. However, in none of the cases examined does it approach -1 or even become noticeably smaller then 0. In fact, the smallest g^{RT} value is equal to -0.012 and corresponds to type 1 inclusions and the extreme scattering optical thickness $\tau = 25$. As a consequence, the total asymmetry parameter values are always positive and never drop below 0.492.

Paper 2 suggests that the ray-tracing asymmetry parameter can be reduced significantly by increasing absorption inside the composite particle because in this case it is only the light scattered to the sides and rear by the inclusions near the back-facing surface of the composite particle that readily escapes. However, this mechanism of reducing the ray-tracing asymmetry parameter

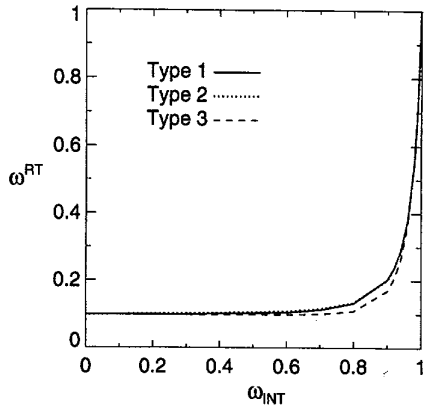

Fig. 3. Ray-tracing single-scattering albedo, ω^{RT}, versus internal single-scattering albedo, ω_{INT}, for a 50 μm diameter host sphere with $m_H = 1.55$, $\tau = 25$, and type 1, type 2, and type 3 inclusions.

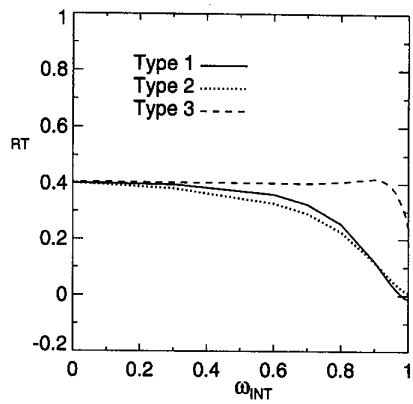

Fig. 4. As in Fig. 3, but for the ray-tracing asymmetry parameter, g^{RT}.

contradicts the results of Hapke's own laboratory measurements.[42] Indeed, Figs. 12–14 of Ref. 42 (phase function measurements for resin spheres with multiple internal inclusions and resin agglutinates)
clearly show that the ray-tracing asymmetry parameter for large composite particles can only be expected to increase with increasing absorption because absorption suppresses the backscattering component of the ray-tracing phase function. This conclusion is fully corroborated by our calculations shown in Plates 3 and 4 and Figs. 3 – 6. Figures 3 and 4 along with Eq. (8) demonstrate that the effect of increasing absorption on the total asymmetry parameter is twofold: absorption not only increases the ray-tracing asymmetry parameter g^{RT}, but also reduces the ray-tracing single-scattering albedo ω^{RT} and, thus, the ray-tracing contribution to the total asymmetry parameter. As Fig. 1 shows, the discrete internal inclusions are strong forward scatterers and relatively weak back scatterers. Therefore, photons refracted into a composite particle need many scattering events to change the direction of propagation and finally exit in the direction opposite to the direction of initial incidence. However, owing to a longer path inside the host medium such photons have a greater probability to be absorbed. Furthermore, in the case of very strong internal absorption the ray-tracing asymmetry parameter is dominated by the positive contribution of rays externally reflected by the particle surface. Therefore, the only way to considerably decrease the ray-tracing asymmetry parameter is to increase the amount of multiple scattering inside the composite particle. This can only be achieved by decreasing rather than by increasing absorption.

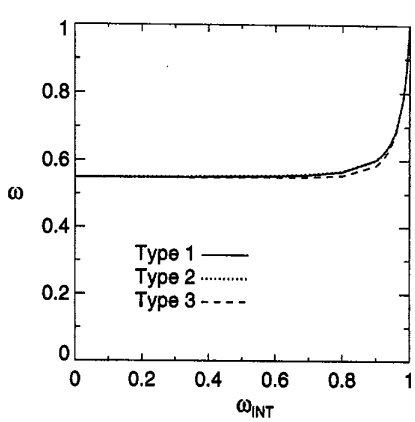

Fig. 5. As in Fig. 3, but for the total single-scattering albedo, ω.

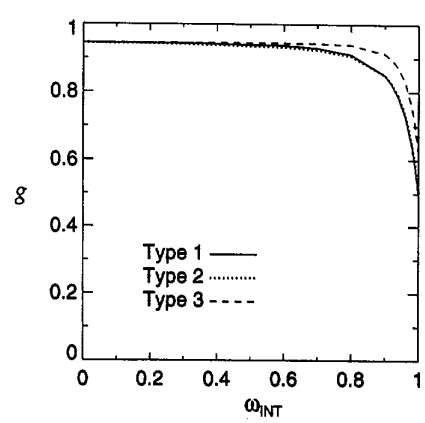

Fig. 6. As in Fig. 3, but for the total asymmetry parameter, g.

Since the refractive index $m_2 = 2$ of type 2 inclusions can be unrealistically high in many cases, we also examined the case of type 3 inclusions with the same effective radius $a = 0.5$ μm but a smaller refractive index, $m_3 = 1.65$. Figures 3 – 6 and Plate 5 display calculations for the scattering optical thickness of the composite particle $\tau = 25$ and the internal single-scattering albedo, ω_{INT}, varying from 1 to 0. These calculations clearly show that the reduced refractive index contrast between the inclusions and the host medium causes significantly increased ray-tracing and total asymmetry parameters, especially for ω_{INT} equal or close to 1. This is an expected result since the phase function for type 3 inclusions has a stronger forward-scattering and a weaker backscattering components than the phase functions for type 1 and type 2 inclusions (Fig. 1).

All calculations discussed so far pertain to the host refractive index $m_{\mathrm{H}} = 1.55$ corresponding to silicates. Another abundant material covering the surfaces of many solar system bodies is water ice, with a refractive index of 1.31 in the visible. Figure 1 shows the phase function for type 4 inclusions (vacuum bubbles with $a = 0.5$ μm and $m_{\mathrm{H}} = 1.31$), while Plate 6 and Fig. 2 show the results of ray-tracing calculations for a 50 μm diameter ice particle with type 4 inclusions, no internal absorption, and scattering optical thicknesses from 0 to 25. Again, the ray-tracing phase function for $\tau = 0$ (no inclusions) exhibits the well-known geometric optics features which rapidly disappear with increasing τ. Figure 2 shows, however, that the ray-tracing asymmetry parameter for the composite ice particle is systematically larger than that for the silicate particle with type 1 inclusions, and the minimum g^{RT} value for the ice particle with $\tau = 25$ (corresponding to 29,506 internal vacuum bubbles) is close to $+0.124$, in contrast to the minimum value $g^{\mathrm{RT}} = -0.012$ for the optical-thickness-equivalent silicate particle. This result can be easily explained by the fact that the phase function for vacuum bubbles in ice is less backscattering than that for vacuum bubbles in the silicate host medium (Fig. 1) and that, generally, homogeneous particles with a lower refractive index (ice) tend to be more forward-scattering than those with a larger refractive index (silicate). It thus appears that it is more difficult to make an ice particle backscattering by filling it with multiple voids than a silicate particle.

3. DENSELY PACKED LARGE COMPOSITE PARTICLES

We have shown in the preceding section that multiple internal inclusions cannot make the total asymmetry parameter for a large isolated particle negative. As discussed in Paper 1, another scattering mechanism that can reduce the asymmetry parameter is high packing density. Although it is doubtful that large heterogeneous particles can be considered as elementary, single scatterers when they are densely packed (see Sec. 4.2), in this section we adopt this assumption of Paper 2 and compute the asymmetry parameter for densely packed particles with inclusions by using the static structure factor theory as summarized in Paper 1.

It should be emphasized here that according to the qualitative discussion of Refs. 12 and 20, the extinction and scattering cross-sections and the phase function of regolith particles covering planetary surfaces completely lack a diffraction component whatever the value of the filling factor, f (i.e., the fraction of volume occupied by the particles). In other words, it is claimed that for any $f \neq 0$ the extinction and scattering cross-sections, the phase function, and the asymmetry parameter for closely spaced scatterers are identical to their respective geometric optics components. It is clear, however, that the diffraction contribution to the extinction cross-section is a function of f and varies from 50% at $f = 0$ to 0% at $f = 1$, and that there is no critical filling factor value before which the diffraction contribution is equal to 50% and after which it suddenly drops to 0%. The same is true of the scattering cross-section, the phase function, and the asymmetry parameter. Unlike the qualitative discussion of Refs. 12 and 20, the theory based on the introduction of the static structure factor allows one to quantify the effect of packing density on the diffraction contribution and to verify whether the only non-zero components of the scattering characteristics of regolith particles are the geometric optics ones. The quantitative analysis of the dependence of the light scattering characteristics on packing density is very important since, for natural surfaces, the filling factor can vary from a few per cent (e.g., for snow and frost surfaces) to several tens of per cent.

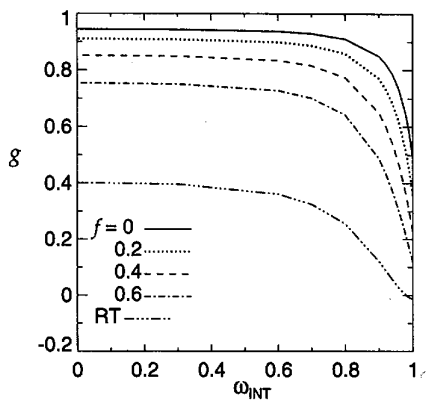

Fig. 7. Total asymmetry parameter versus internal single-scattering albedo for densely packed 50 μm diameter composite particles with $m_H = 1.55$, $\tau = 25$, and type 1 inclusions. The fraction of volume occupied by the composite particles varies from $f = 0$ to 0.6. For comparison, the ray-tracing asymmetry parameter, g^{RT}, for an isolated composite particle is also shown.

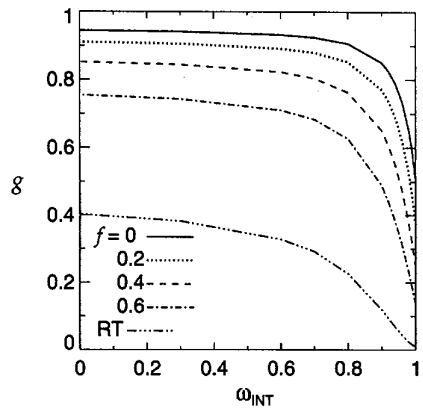

Fig. 8. As in Fig. 7, but for type 2 inclusions.

By using formulas of Paper 1, it is easy to show that the asymmetry parameter for densely packed particles is expressed in terms of the phase function of a single isolated particle $p(\Theta)$ as follows:

$$g = \frac{\int_{-1}^{1} \mathrm{d}(\cos\Theta) S(\Theta) p(\Theta) \cos\Theta}{\int_{-1}^{1} \mathrm{d}(\cos\Theta) S(\Theta) p(\Theta)}, \tag{11}$$

where $S(\Theta)$ is the static structure factor which depends not only on the scattering angle Θ, but also on the particle size parameter $x = \pi D/\lambda$ and filling factor f. The static structure factor can be computed by using Eqs. (7)–(15) of Paper 1. The isolated-particle phase function for a large composite scatterer is given by Eq. (7) and is computed as described in Sec. 2. The integrals in Eq. (11) are evaluated numerically by using a Gaussian quadrature formula with a large number of division points.

Figures 7 – 9 show the results of calculations for densely packed, 50 μm diameter composite particles with the host refractive index $m_H = 1.55$, scattering optical thickness $\tau = 25$, internal single-scattering albedo ω_{INT} varying from 0 to 1, and type 1, type 2, and type 3 inclusions. The wavelength is 0.55 μm and the fraction of volume occupied by the large composite particles

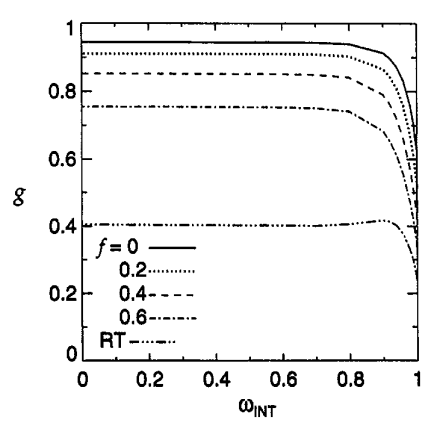

Fig. 9. As in Fig. 7, but for type 3 inclusions.

increases from 0 (widely separated particles) to 60% (extremely high packing density). It is seen that increasing filling factor indeed results in a decrease of the asymmetry parameter. However, in all the cases examined the asymmetry parameter remains positive despite the extremely high values of the filling factor and the internal scattering coefficient of the composite particles. The smallest g values for particles with type 1, type 2, and type 3 inclusions and $f = 0.6$ are equal to 0.118, 0.137, and 0.337, respectively, and are reached in the limit of zero absorption ($\omega_{\mathrm{INT}} = 1$). The respective smallest g value for non-absorbing 50 μm diameter ice particles with $f = 0.6$, type 4 inclusions (micrometre-sized vacuum bubbles), and $\tau = 25$ is equal to 0.236. Furthermore, Figs. 7 – 9 show that even modest absorption sharply increases the asymmetry parameters and makes the large, densely packed composite particles moderately and even strongly forward-scattering. For comparison, Figs. 7 – 9 also show the respective ray-tracing asymmetry parameters computed for isolated composite particles. Not surprisingly, our computations (not shown here) indicate that the effect of packing density on the nearly isotropic or moderately anisotropic ray-tracing component of the phase function is negligible. Therefore, Figs. 7 – 9 demonstrate that, contrary to Ref. 12, even high packing density does not completely suppress the diffraction component of the phase function and does not reduce the total asymmetry parameter to the ray-tracing one. In fact, packing density barely affects the diffraction asymmetry parameter [see the middle column of Table 2 which shows the result of applying Eq. (11) to the diffraction phase function of Eq. (3)] and influences the diffraction contribution to the total asymmetry parameter only by reducing the diffraction cross-section (see below).

Assuming that the absorption cross-section is not modified by the effect of packing density,[10] it is straightforward to show that the single-scattering albedo for densely packed composite particles is expressed in terms of their ray-tracing single-scattering albedo as follows:

$$\omega(f) = \frac{(1 + \omega^{\mathrm{RT}})B(f)}{(1 + \omega^{\mathrm{RT}})B(f) - \omega^{\mathrm{RT}} + 1}, \tag{12}$$

where

$$B(f) = \frac{C_{\mathrm{sca}}(f)}{C_{\mathrm{sca}}(f = 0)} = \frac{1}{2}\int_{-1}^{1} \mathrm{d}(\cos\Theta)p(\Theta)S(\Theta) \tag{13}$$

is the ratio of the scattering cross-section of densely packed particles to that of isolated particles. Figures 10 – 12 show that increasing packing density decreases the single-scattering albedo. This is an expected result because packing density affects the diffraction component of the scattered light more strongly than the less anisotropic ray-tracing component and makes the diffraction scattering cross-section significantly smaller than the particle geometric cross-section [see Table 2 which tabulates the result of applying Eq. (13) to the phase function of Eq. (3)]. However, Figs. 10 – 12 clearly demonstrate that it is wrong to assume[12, 20, 42] that the single-scattering albedo of large densely packed particles is equal to their ray-tracing single-scattering albedo.

Paper 2 calls computations of Paper 1 based on the structure factor theory an important contribution since they allow one to quantify the effect of packing density on the diffraction component of the differential scattering cross-section. The calculations show that increasing packing density results in significant changes in the optical cross-sections, single scattering albedo, and asymmetry parameter. However, contrary to the postulate of Refs. 12 and 20, the effect of packing density is never equivalent to just subtracting the diffraction component completely and retaining only the ray-tracing component. Furthermore, even if that postulate were true, the ray-tracing computations of Sec. 2 show that one needs a combination of an unrealistically large

Table 2. Diffraction asymmetry parameter g^{D} and ratio B^{D} of the diffraction scattering cross-section to the geometric cross-section versus filling factor f for densely packed 50 μm diameter spheres. The wavelength is 0.55 μm.

f	g^{D}	B^{D}
0	0.998	1
0.2	0.996	0.584
0.4	0.993	0.314
0.6	0.985	0.150

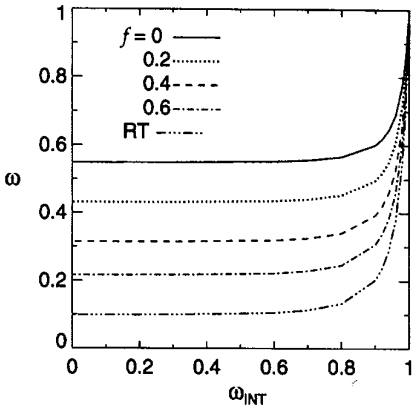

Fig. 10. Total single-scattering albedo versus internal single-scattering albedo for densely packed 50 μm diameter composite particles with $m_H = 1.55$, $\tau = 25$, and type 1 inclusions. The fraction of volume occupied by the composite particles varies from $f = 0$ to 0.6. For comparison, the ray-tracing single-scattering albedo, ω^{RT}, for an isolated composite particle is also shown.

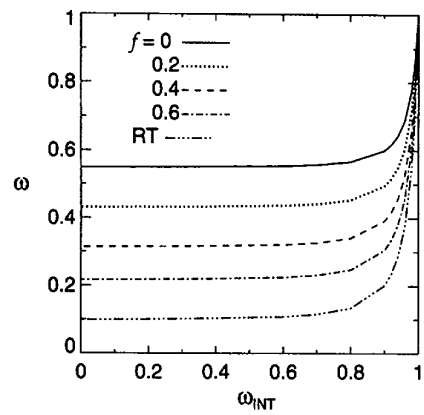

Fig. 11. As in Fig. 10, but for type 2 inclusions.

scattering optical thickness, a very large refractive index contrast between the inclusions and the host medium, and no internal absorption in order to make the ray-tracing asymmetry parameter for a composite regolith particle even slightly negative. The results of Refs. 43 and 44 suggest that this combination is unlikely to be encountered in nature.

4. DISCUSSION

The results of theoretical computations reported in Secs. 2 and 3 clearly show that it is essentially impossible to make regolith particles backscattering by filling them with large numbers of internal inclusions in the form of voids and/or grains with a refractive index different from that of the host medium. The computed asymmetry parameters remain positive even for densely packed composite particles with no internal absorption and extreme values of the filling factor and internal scattering coefficient. Furthermore, they are sharply increased by even modest absorption inside the composite particle and/or by reducing the refractive index contrast between the internal inclusions and the host medium. Also, comparison of Figs. 12–14 of Ref. 42 demonstrates that the model of composite particles with a large number of small discrete inclusions overstates the effect of internal structure on the asymmetry parameter of agglutinate particles. The same conclusion follows from laboratory phase function measurements for large, highly heterogeneous terrestrial and meteoritic particles.[43] The phase functions measured in Ref. 43 exhibit a shallow minimum at

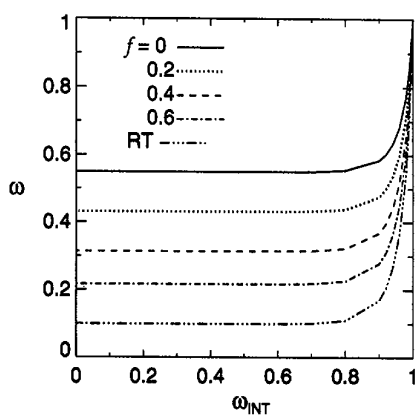

Fig. 12. As in Fig. 10, but for type 3 inclusions.

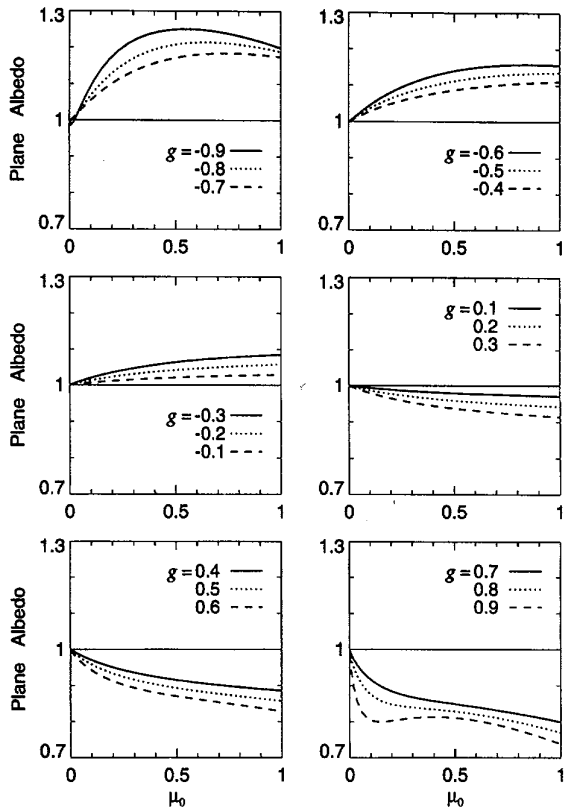

Fig. 13. Plane albedo versus cosine of solar zenith angle computed with the Hapke BRF for the Henyey–Greenstein phase function with the asymmetry parameter varying from -0.9 to 0.9 and the single-scattering albedo equal to 1. Note that for $g = 0$, $A_P(\mu_0) \equiv 1$.

side-scattering angles, a broad backscattering maximum with an enhancement by a factor of 1.5–2 over the minimum, and a narrower and (much) stronger forward-scattering peak. The minimal scattering angle in those measurements is 20° so that the even stronger forward-scattering diffraction peak does not show up and the measurements demonstrate only the ray-tracing part of the phase function. However, even the ray-tracing part of the phase function is strongly forward-scattering and definitely has a positive asymmetry parameter. Quite similar, strongly forward-scattering phase functions have been retrieved by Lamy and Perrin[44] for interplanetary dust particles. Altogether, this body of evidence suggests that the negative asymmetry parameters

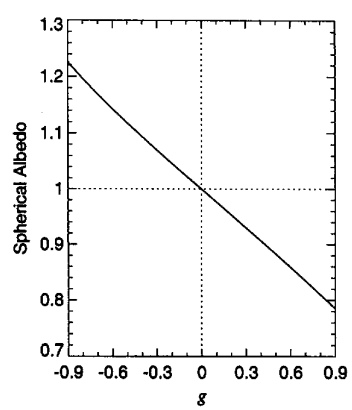

Fig. 14. Spherical albedo versus asymmetry parameter computed with the Hapke BRF for the Henyey–Greenstein phase function and the single-scattering albedo equal to 1.

obtained with the Hapke bidirectional reflection function (BRF) for regolith grains are physically unrealistic. In view of our results, the evidence for the smallest asymmetry parameter reported in Ref. 23 ($g = -0.6$) is especially weak since it was retrieved for strongly absorbing particles with $\omega = 0.204$. Also, the computations shown in Figs. 10 – 12 suggest that a single-scattering albedo as low as 0.037 (and accompanied by an asymmetry parameter as small as -0.47)[22] may be another artefact of applying the model BRF to planetary observations. Thus, we have to conclude that the negative asymmetry parameters retrieved with the model for regolith grains need another explanation rather than assuming that they are real and result from the complete disappearance of diffraction and a complicated internal structure of the particles.

4.1. The Hapke model

As mentioned above, the concept of backscattering particles has been invoked to justify the negative asymmetry parameters retrieved with the Hapke model. However, as has been shown in Paper 1, these negative asymmetry parameters may be just an artefact of using an approximate phenomenological approach in trying to solve an ill-conditioned inverse scattering problem. That the problem of retrieving the asymmetry parameter of the phase function from remotely sensed bidirectional reflectance measurements is indeed ill-posed is illustrated by the following example. It is well known that, for particles with sizes much larger than the wavelength of light, there is a sharp forward-scattering diffraction peak in the single-scattering phase function.[1] This peak necessitates a large number of terms in the Fourier decomposition of the phase function and a large number of angular quadrature points in computing multiple light scattering by using, e.g., the adding/doubling method. However, as was demonstrated by Hansen[45] and Hansen and Pollack[46] on the basis of exact radiative transfer computations, the photons scattered into the forward peak can be approximated as being unscattered by truncating the diffraction peak from the phase function and appropriately reducing the single-scattering albedo and optical thickness. Obviously, no renormalization of the optical thickness is required for a semi-infinite medium. It has been found that this approximation produces errors in the computed reflection function not exceeding several per cent for many scattering geometries (except forward-scattering geometries with nearly grazing incidence and reflection). Thus, a strongly forward-scattering phase function and a nearly isotropic phase function produce similar reflectivities of a semi-infinite medium provided that the single-scattering albedo for the latter phase function is reduced and extreme forward-scattering geometries are avoided. Therefore, we must conclude that the reflectance of an optically thick medium can be almost insensitive to the presence of the forward-scattering phase function peak.

This example demonstrates that large changes in the phase function, when compensated for by reducing the single-scattering albedo, can result in negligibly small changes in the reflectance. As a consequence, measurement errors and/or approximations made in computations of radiative transfer can result in big errors in the retrieved single-scattering phase function unless additional information is used to reject unphysical solutions.

The use of the truncated phase function in multiple-scattering computations is justified if one realizes that the real phase function is forward-scattering and the truncation approximation is employed only to speed up computer calculations. However, if someone *interprets* the results of such computations as evidence that the real phase function is nearly isotropic and derives further conclusions from this interpretation, it becomes a crude distortion of the real physical situation.

Besides the opposition-effect term, the Hapke model of bidirectional reflectance is nothing more than an approximate solution of the radiative transfer equation. The approximation, which is always made in the model regardless of the actual single-scattering phase function, is replacing the rigorous multiple-scattering term by that for isotropic scatterers. The simplification which is employed almost always is approximating the first-order-scattering contribution by a single-term Henyey–Greenstein phase function or a few-terms expansion in Legendre polynomials. Although the second approximation can, in principle, be relaxed, it is this approximation that has always been made in retrieving the negative asymmetry parameters of the phase function from real measurement data (see Refs. 12, 22, 23, 47, 48 and references therein). Thus, the Hapke model, as it stands now, does not provide a self-consistent means to compute theoretically the reflectivity of a particulate surface starting with physically correct single-scattering calculations for particles of a given size, shape, refractive index, internal structure, and compaction state and finishing by

accurate computations of multiple scattering. Instead, the model declares the asymmetry parameter of the phase function and the single-scattering albedo free model parameters, and their values are determined only by fitting reflectance data. As a consequence, the quality of the fit rather than a physical constraint is the only measure of the ability of the model to describe the reality. This approach to analyzing data can at best be called phenomenological.

It should be emphasized again that Paper 1 criticizes the Hapke model not only for using the isotropic multiple-scattering term, but also for using simplified and unrealistic phase functions in analyzing real experimental data. The latter means that instead of computing the phase function based on the morphology and composition of the scattering medium and using a relevant physical theory, a phase function of a particular kind is postulated and its formal parameters are determined by fitting the data. However, the ultimate proof of the relevance of a bidirectional reflectance theory is the comparison of model computations with results of controlled laboratory experiments. In the case of the Hapke model this comparison is impossible because the size distribution, shape, refractive index, internal structure, and compaction state of regolith particles are not explicit model parameters.

The deficiency of the phenomenological approach is vividly demonstrated by the application of the model to Venus observations.[47,49] Figures 3 and 4 of [49] and Fig. 9 of [47] show an almost perfect fit of model computations to relative brightness profiles of the Venus atmosphere obtained with an asymmetry parameter equal to zero. This result indicates the absence of clouds in the Venus atmosphere (the asymmetry parameter zero corresponds to a purely gaseous atmosphere), whereas it is well known that the whole planet is covered with an optically thick cloud layer composed of strongly forward-scattering particles with a large positive asymmetry parameter of about 0.7–0.8 in the visible.[50] Paper 2 asserts that this example is irrelevant since "all it demonstrates is the obvious: that a particle phase function cannot be retrieved from data taken at a single phase angle". However, despite the obviousness, the excellent fit of the model computations to the observational data and the disability of the model to reject unphysical solutions caused Hapke to erroneously claim that the Venus atmosphere has an additional component which is isotropically scattering and weakly polarizing.[49] Furthermore, Fig. 9 of Ref. 47 has been reproduced in a recent book[20] as an example of the ability of the model to describe bidirectional reflectance of real scattering media.

Another example of the inability of the phenomenological approach to adequately retrieve the asymmetry parameter is the application of the model to analyzing reflectance measurements of a cobalt glass powder (Fig. 3 of Ref. 47). As the last row of Table 1 of Ref. 47 shows, the model makes the phase function for almost non-absorbing, transparent glass particles backscattering (model asymmetry parameter $g = -b/3 = -0.24$). This is physically meaningless even if one assumes that the glass particle phase function lacks the diffraction component completely, which is never the case. The explanation of this model artefact is simple. The isotropic multiple-scattering term adopted in the model can significantly underestimate the real contribution of multiple scattering in the backward direction. To compensate for this underestimation, the model artificially enhances the backward component of the single-scattering phase function, thus reducing the asymmetry parameter and even making it negative.

Our example with truncating the forward-scattering component of the phase function and renormalizing the single-scattering albedo suggests that this may be exactly what the Hapke BRF is forced to do when its isotropic multiple-scattering term fails to reproduce the actual multiple-scattering component of the reflection function. To match the measured reflectance, the approximate BRF artificially truncates the forward-scattering component of the phase function and decreases the single-scattering albedo, thus considerably reducing the amount of multiple scattering. This, in turn, necessitates an increased backscattering component of the model phase function. As a result, the model asymmetry parameter becomes substantially smaller than the actual value and even negative. Therefore, it comes as no surprise that when Helfenstein et al[51] used a more accurate technique for computing multiple scattering and allowed more complex phase functions than a single-term Henyey–Greenstein phase function, they were able to fit lunar photometric data with a forward-scattering phase function and a larger single-scattering albedo than that retrieved with the standard Hapke BRF.

Unfortunately, since its formulation, the approximate BRF has not been thoroughly tested against rigorous computations of radiative transfer. Our comparisons with accurate radiative

transfer calculations show that it can produce unacceptably large errors exceeding 100% at forward-scattering geometries. Paper 2 (p. 838) asserts that the model BRF is still useful, even though it is inexact, because of the large observational errors inherent in planetary reflectance measurements. In this regard, Paper 2 claims that it is difficult to carry out absolute planetary photometry to much better than $\pm 10\%$. This is not true. For example, the absolute radiometric accuracy of the Galileo Photopolarimeter/Radiometer instrument is $\pm 3\%$ with precision better than 1%.[52] Similarly high is the photometric accuracy of the French Polarization and Directionality of the Earth's Reflectances instrument[53] as well as of NASA Earth Observing System instruments such as the Moderate Resolution Imaging Spectrometer,[54] Multi-Angle Imaging Spectro-Radiometer,[55] and the Earth Observing Scanning Polarimeter.[56] It is quite clear that this accuracy is unattainable with the approximate model BRF, which makes it essentially useless for remote sensing purposes. Moreover, the application of the model to natural snow surfaces[48] and to Venus observations[57] shows that even the best-fit curves deviate from experimental data by more than 50 and 40%, respectively. In both cases the largest errors are found at small scattering angles and are undoubtedly the result of using the isotropic multiple-scattering term.

Since it is clear that the model BRF is prone to significant errors, it is important to at least make sure that these errors do not lead to a serious violation of fundamental physical laws. Two such fundamental laws which must be obeyed by any bidirectional reflection function are the reciprocity principle and the energy conservation law. The reciprocity principle requires that any bidirectional reflection function R be symmetric with respect to the directions of light incidence and reflection:[58]

$$R(\mu,\varphi;\mu_0,\varphi_0) = R(\mu_0,\varphi_0;\mu,\varphi)\,, \tag{14}$$

where the cosine of the zenith angle μ and the azimuthal angle φ specify the direction of light reflection and the same quantities with the subscript 0 specify the direction of the incident beam. The energy conservation law requires that for a semi-infinite medium composed of arbitrary non-absorbing scatterers, the plane albedo $A_{\mathrm{P}}(\mu_0)$ and the spherical albedo A_{S} be identically equal to unity. The plane and the spherical albedos are defined by the following formulas:[59]

$$A_{\mathrm{P}}(\mu_0) = \frac{1}{\pi}\int_0^{2\pi} \mathrm{d}\varphi \int_0^1 \mathrm{d}\mu\mu R(\mu,\varphi;\mu_0,\varphi_0)\,, \tag{15}$$

$$A_{\mathrm{S}} = 2\int_0^1 \mathrm{d}\mu_0\mu_0 A_{\mathrm{P}}(\mu_0)\,. \tag{16}$$

It is well known that exact solutions of the radiative transfer equation (e.g., the adding/doubling solution) satisfy both conditions.[59] Hapke's BRF is constructed such that it obeys the reciprocity principle. However, this BRF inherently violates the energy conservation law. Figures 13 and 14 show the plane and the spherical albedos computed for the Henyey–Greenstein phase function,

$$p_{\mathrm{HG}}(\Theta) = \frac{1-g^2}{(1-2g\cos\Theta+g^2)^{3/2}}\,, \tag{17}$$

with the asymmetry parameter g varying from -0.9 to 0.9. Note that we have computed the isotropic multiple-scattering term accurately rather than by using Hapke's[12] approximation for Chandrasekhar's H-functions. It is seen that the model BRF "emits" extra energy for backscattering phase functions and "absorbs" extra energy for forward-scattering phase functions, the amount of the "extra" energy being as large as $+25\%$ for $g = -0.9$ and -26% for $g = 0.9$ (Fig. 13). These "phantom" energy excess and energy deficit are absolutely unphysical and result from using the isotropic multiple-scattering term in the model BRF regardless of the actual phase function. One can expect that the albedo differences between the model BRF and the exact solution of the radiative transfer equation decrease with decreasing single-scattering albedo. However, for non-absorbing or weakly absorbing scattering media, the model produces physically meaningless results. For example, the model yields the asymmetry parameter $+0.79$ for a surface frost sample analyzed in Ref. 48. This means that the model predicts that this high-albedo sample absorbs as much as 20% more energy than it really does (Fig. 13). The same is true for the Venus cloud layer

if its radiation balance is calculated with the Hapke model and the true cloud particle phase function (cf. Ref. 57). Needless to say, reflecting 15–20% less solar energy would have made the Venus atmosphere much different from what it is now. Note that the plane and the spherical albedos are integral scattering characteristics, and the model errors in A_P and A_S shown in Figs. 13 and 14 are angular integrals over the errors at particular scattering geometries. Therefore, the errors for individual scattering geometries are expected to be even (much) larger.

A numerical example given in Paper 1 clearly shows that the phenomenological Hapke model is capable of retrieving a negative asymmetry parameter for strongly forward-scattering particles. Paper 2 questions the relevance of that example by giving another example based on calculations for a linear anisotropic phase function,

$$p(\Theta) = 1 + a \cos \Theta \tag{18}$$

with $a = +1$ and -1. Unfortunately, this choice of the phase function can hardly be considered realistic. First, it is highly unlikely that real phase functions can be represented by a two-term Legendre expansion. Second, the non-negativeness of the phase function requires that the absolute value of the asymmetry parameter $g = a/3$ be less than or equal to 1/3: $|g| \leq 0.333\ldots$ Thus, contrary to what is claimed in Paper 2, one is dealing with weakly anisotropic scattering whatever is the value of the parameter a. Third, Paper 2 considers only the case of conservative scattering ($\omega = 1$). However, close inspection of chapter 46 of Ref. 60 shows that this choice of the single-scattering albedo and phase function makes the reflection function for $\mu = 1$ or $\mu_0 = 1$ (perpendicular incidence or perpendicular reflection, respectively) independent of a. In other words, this example is based on a mathematical singularity which disappears when a more realistic phase function is chosen (Paper 1) or non-conservative scattering is considered. However, even this peculiar example demonstrates the need to avoid using an approximate BRF. Indeed, if we use the exact solution of the radiative transfer equation with the phase function of Eq. (18) to analyze Fig. 5(A) of Paper 2, we have to conclude that the inverse problem has no unique solution since all a from the interval $[-1, 1]$ produce the same reflectivity. This means that we are warned about the ill-conditionality of the inverse problem and should not make any conclusions about the actual value of a. In contrast, the use of the model BRF suggests that the problem is well defined and produces a unique solution, $a = 0$. Indeed, since the isotropic multiple-scattering term gives wrong values of the multiple-scattering contribution to the reflection function for all a but $a = 0$, the model can match the curve in Fig. 5(A) of Paper 2 only with $a = 0$.

Paper 2 also mentions a work by Goguen[61] who measured the bidirectional reflectance of a layer of glass microspheres with known size and refractive index and then tried to reproduce the measurement results by using the adding/doubling solution of the radiative transfer equation and Hapke's BRF. It is true that neither the adding/doubling solution nor the model BRF provided a perfect fit and that the model gave a better agreement in some cases. However, from the scientific standpoint it would be more appropriate to discuss what factors were not taken into account in Goguen's radiative transfer computations rather than to claim that the approximate reflection function is, inexplicably, a more accurate solution of the radiative transfer equation than the exact adding/doubling solution. For example, it is likely that the standard assumption of a continuous medium traditionally made in the radiative transfer theory is reasonably accurate deeply inside the medium but is violated near the boundaries where the effect of random fluctuations of particle positions on the reflected intensity is much stronger. Also, it is obvious that reflectance at oblique incidence and reflection is strongly affected by the microscopic surface roughness on the scale of a few or several particle diameters. Another factor can be the modification of the phase function by the effect of packing density. These three factors might explain the residual differences between measurements and adding/doubling calculations at larger phase angles (the phase angle is defined as 180° minus the scattering angle). The influence of both factors should be minimal at phase angles close to zero. And indeed, the results of Goguen (especially those not mentioned in Paper 2) demonstrate much better agreement between laboratory data and adding/doubling computations at small phase angles than between the data and the model BRF. The discrepancy between the laboratory measurements and the model BRF at small phase angles is unambiguously explained by the inability of the isotropic multiple-scattering term to reproduce the actual contribution of multiply scattered light. Importantly, the results of Goguen[61] are in agreement with the results of

Jones et al[62] who also compared controlled laboratory measurements of intensity exiting a densely packed bed with standard radiative transfer calculations. Jones et al have concluded that radiative transfer near the boundaries of the medium might not be adequately represented by a continuous form of the radiative transfer equation, and that a non-continuous radiation model accounting for spatial features in detail may be necessary to model radiation intensity near the medium boundaries.

Microscopic surface roughness on the scale of a few or several particle diameters is a factor the importance of which is completely ignored in Paper 2. Paper 2 claims that the only way to explain the phase dependence of the lunar reflectivity with a forward-scattering regolith particle phase function is to assume that the lunar surface is macroscopically rough. Paper 2 further asserts that explanations invoking macroscopic surface roughness are inadequate because in the laboratory, where the surfaces of samples are macroscopically smooth, lunar soils are still found to be backscattering. However, the reflectance data of Goguen,[61] obtained at exactly the same scattering geometry as Fig. 1 of Paper 2 but for non-absorbing, clear glass spheres, show that microscopic surface roughness suppresses the effect of the forward-scattering component of the phase function on the reflectance at large phase angles and, thus, makes the strongly forward-scattering glass particles look backscattering. Obviously, this effect of microscopic surface roughness is even stronger for absorbing lunar soils.

As Paper 1 points out, the determination of the asymmetry parameter from reflectance measurements is an ill-conditioned inverse problem. Therefore, experimental noise and approximations made in theoretical computations can result in an excellent fit with a wrong value of the asymmetry parameter. As a consequence, the approximations made in Hapke's phenomenological model and the intrinsic inability to reject unphysical solutions can make the model BRF nothing more than an interpolation tool, and the model asymmetry parameter nothing more than a free coefficient of the interpolation function rather than a physically meaningful quantity. The model BRF might be useful as an interpolation function if it is utilized only to fit the data, and no questions are asked as to the physical meaning of the retrieved formal model parameters. However, the formal model parameters should not be associated with real physical quantities if this fit is used to derive information about the structure of the scattering medium.

Paper 2 correctly points out that broadening the range of scattering angles covered by measurements can improve the accuracy of retrieving the particle phase function and asymmetry parameter. However, it is not clear why the range of phase angles should be extended to *at least* 120°, as Paper 2 suggests. Figure 3 of Paper 2 clearly shows that in order not to miss the forward-scattering ray-tracing peak and, especially, the narrow forward-scattering diffraction peak and, thus, not to declare forward-scattering particles backscattering, the range of phase angles should be extended up to 180°. Furthermore, even if the range of scattering angles is broad, the effect of the forward-scattering component of the phase function on the reflection function at large phase angles is hard to separate from the effects of microscopic and macroscopic surface roughness, and physical constraints may still be necessary to reject wrong solutions. Therefore, any computations of radiative transfer must be based on physically correct single-scattering computations. Such a self-consistent physical approach is described in standard textbooks on remote sensing.[63–66] Paper 2 claims that because phase functions of regolith particles at phase angles beyond about 150° are hard to measure, it is rank speculation to insist that they are forward-scattering. This is true unless a physically based constraint is used to select the correct value of the asymmetry parameter. Therefore, the results of Paper 1 and this paper strongly suggest that it is rather rank speculation to intuitively insist that the regolith particle asymmetry parameters can indeed be negative. Moreover, spacecraft-remote-sensing measurements of the earth and planets are often confined to a much narrower range of phase angles than [0°, 150°] and, in most cases, pertain to nearly backscattering geometries. This factor even further enhances the importance of the self-consistent physical approach to analyzing experimental data. As the results of [50, 67–69] show, measuring polarization as well as intensity of the reflected sunlight can provide an additional physical constraint that helps to ameliorate the non-uniqueness problem in remote-sensing retrievals.

After all, at present there is no reason to use an approximate solution of the radiative transfer equation, especially if it is known to be capable of producing non-physical results. Today one has access to advanced and extremely efficient methods for numerically solving the radiative transfer

Fig. 15. Light scattering by widely separated particles. This figure demonstrates that the scattering angle can be unambiguously defined as the angle between the incident beam and the line connecting particles A and B.

equation (with and without account of polarization) with high accuracy,[1, 70–74] and these methods can be readily implemented on moderate workstations and PCs. In this regard, the statement that computing Fig. 6 of Paper 2 takes 30 h of CPU time on a SUN SPARC workstation (p. 847 of Paper 2) is misleading. Indeed, with the software that we have and which is based on exactly solving the radiative transfer equation for an optically semi-infinite medium,[70, 73] the computation of the same scattering model on an IBM RISC model 37T workstation took less than 10 min of CPU time when the full Stokes reflection matrix was calculated and well less than 1 min when only the reflected intensity was computed. Needless to say, the Hapke model cannot even be claimed to be able to adequately describe the multiple scattering of polarized light.

4.2. Elementary scatterers in a medium consisting of densely packed composite particles

One of the main assumptions made in Paper 2 is that the dominant optical characteristic of most regolith particles is their strong heterogeneity. Paper 2 further claims that large composite particles remain single, elementary scatterers even when they become densely packed, so that the retrieved negative values of the single-scattering asymmetry parameter must be associated with the composite particles rather than with their components. However, this is not the case, as is explained below. In this explanation, we assume that particles are much larger than the wavelength so that the geometric optics concept of light rays is applicable. The radiative transfer equation operates with a quantity called the phase function which describes the angular distribution of the intensity of light scattered by a particle. The phase function is a function of the scattering angle, i.e., the angle between the incident and the scattered beams. For an individual particle viewed from a distance much larger than the particle size, the scattering angle can be uniquely defined. Indeed, as shown in Fig. 15, individual rays exiting different parts of particle A come to a remote observation point (particle B) within a very small solid angle and almost overlap, and the scattering angles for the individual rays essentially coincide. Therefore, the scattering angle can be unambiguously defined as the angle between the incident beam and the line connecting any point inside particle A and the observation point. However, when the same particle (particle A) is viewed from a distance comparable to or smaller than its size [Fig. 16(a)], the rays exiting different parts of the particle towards a nearby observation point come to this point within a very large solid angle, the scattering angles for different rays are dramatically different (less than 90° for ray 1 and almost 180° for ray 2), and it is impossible to define a scattering angle for the particle as a single scatterer. Figures 16(a) and 16(b) illustrate the geometry of light scattering in a medium composed of densely packed large particles. It is clearly seen that the scattering angles are different for the individual rays exiting different parts of particle A and illuminating the same part of particle B [Fig. 16(a)]. Moreover, the scattering angles are also different for the individual rays exiting the same part of particle A and illuminating different parts of particle B [Fig. 16(b)]. The difference between the sparse-medium configuration of Fig. 15 and the dense-medium configuration of Fig. 16 is further emphasized by the fact that all rays scattered by particle A towards particle B in Fig. 16 do not impinge on particle B in Fig. 15.

Thus we have to conclude that whatever their morphology, sparsely distributed large composite particles can be characterized by a scattering phase function which depends on an unambiguously defined scattering angle, whereas the very concepts of the scattering angle and the phase function for the same but closely spaced particles are meaningless.

From the geometric optics standpoint, a photon changes the direction of propagation (i.e., gets scattered) only when it encounters an interface separating two media with different refractive

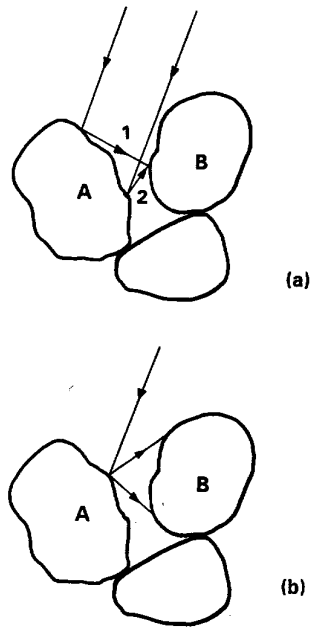

Fig. 16. Light scattering by densely packed particles. This figure demonstrates that the scattering angle cannot be uniquely defined when the distance between large scattering particles is smaller than or comparable to their size.

indices or a small (wavelength-sized or subwavelength-sized) inclusion with refractive index different from that of the host medium.† The exact scattering characteristics of an interface separating medium 1 and medium 2 depend on the ratio of the refractive index of medium 1 to the refractive index of medium 2. However, there is no qualitative difference between an interface separating vacuum and a material medium and an interface separating two material media with different refractive indices because both interfaces cause a beam of light to get scattered. Furthermore, the scattering characteristics of an interface separating a particle and vacuum between regolith particles are identical to those of an interface separating a particle and a vacuum void inside the particle. When a sunlight beam impinges on a planetary surface, it encounters a spatial distribution of interfaces and small inclusions. The interfaces and the small inclusions cause an incident photon to undergo a random walk which ends when the photon finally exits the regolith layer (i.e., gets reflected) or is absorbed inside the layer. This is schematically shown in Fig. 17, in which the random photon trajectories inside the large regolith particles are caused by internal inhomogeneities.

According to Paper 2 (pp. 840 and 841), Paper 1 states that the scattering properties of the three media shown in Fig. 2 of Paper 2 should be identical. However, it is easy to verify by inspection that Paper 1 does not contain such a statement. As was pointed out above, the scattering properties of an interface or a small inclusion depend on the relative refractive index and, thus, depend on the morphology of the medium. The morphologies of the three media shown in Fig. 2 of Paper 2 are different. Therefore, their scattering properties are also different. However, these differences do not make densely packed large composite particles elementary, individual scatterers and provide no way of uniquely defining a phase function for such particles. The elementary scatterers are still small inclusions and interfaces separating any media with different refractive indices, no matter whether or not one of the media is vacuum. Therefore, even if one assumes that the Hapke model is capable of accurately retrieving the asymmetry parameter of the single-scattering phase function

†We define an interface as a surface with extent and local radius of curvature (much) larger than the wavelength so that the ray-tracing concepts of refractions and reflections apply. For example, an interface can separate vacuum and the interior of a large particle or two large grains in optical contact. On the other hand, we assume that the surfaces of small (wavelength-sized or subwavelength-sized) inclusions are not resolved by the incident light so that the concepts of refractions and reflections do not apply. Therefore, from the ray-tracing standpoint, the small inclusions act like point scatterers and their scattering properties are given by Mie theory.

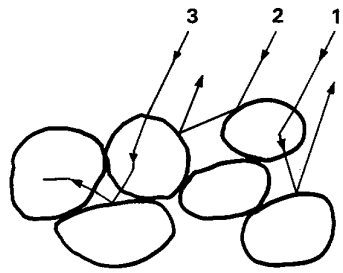

Fig. 17. Random walk of photons in a medium composed of densely packed, large, heterogeneous particles. The broken photon trajectories inside the large particles are caused by internal inhomogeneities. Photons 1 and 2 escape the medium, whereas photon 3 is absorbed inside the medium.

and that the primary optical characteristic of large regolith particles is their strong heterogeneity, the model asymmetry parameter must be associated with the single, elementary scatterers in the form of interfaces and small inclusions rather than with the large regolith particles. However, the retrieved negative asymmetry parameters are still physically unrealistic since both the interfaces and the small inclusions are strong forward-scatterers.

An obvious morphological characteristic of media composed of large, heterogeneous, densely packed particles is that the spatial distribution of the elementary single scatterers (interfaces and small inclusions) is highly inhomogeneous. Furthermore, there are several different scales of inhomogeneity ranging from the internal particle heterogeneity to macroscopic surface roughness. This makes doubtful the applicability of the standard radiative transfer theory to such media because it assumes a locally homogeneous distribution of scatterers and simple flat boundary conditions (cf. the results of Refs. 61 and 62) and makes an obvious case for using a discontinuous stochastic radiative transfer theory (e.g., Refs. 75–80). Unfortunately, analytical methods of this theory are very complicated and are difficult to utilize in practice. It thus appears that the only practical tool for computing the bidirectional reflection function for densely packed heterogeneous particles is the ray-tracing Monte Carlo method (Refs. 81–85 and references therein). The advantage of this technique is its conceptual simplicity, obvious relevance to the kind of situation depicted in Fig. 17, and the ability to treat essentially any internal structure and spatial distribution of composite particles and to simultaneously take into account the effects of microscopic and macroscopic surface roughness. The obvious disadvantage of the method is that it does not take into account the effect of diffraction on the bidirectional reflection function.[81–83] Unfortunately, it is unclear at this moment how to supplement the ray-tracing Monte Carlo method with an accurate computation of diffraction. Apparently, the only theoretical approach suggested so far is that by Keller.[86]

Paper 2 agrees that densely packed composite particles in the form of aggregates or chains composed of smaller grains cannot be considered elementary scatterers and suggests two criteria which are supposed to definitively determine whether a composite particle can be considered an elementary, single scatterer even when this particle is part of a densely packed medium. These two criteria are as follows. (1) A composite particle is an elementary scatterer if a light wave can propagate from any point inside the particle to any other internal point by a variety of paths of finite cross-sectional area without going through vacuum. (2) A composite particle is an elementary scatterer if the refractive indices of its constituent sub-particles relative to their immediate surroundings alter when the particle is broken up into the sub-particles. The irrelevance of the first criterion is demonstrated by the following example. Consider a large host particle with refractive index $m_1 \neq 1$ containing a large inclusion with refractive index $m_2 \neq m_1$, as schematically shown in Fig. 18(a). According to the first criterion, this composite particle is an elementary scatterer if $m_2 \neq 1$. However, if the large inclusion is a vacuum void ($m_2 = 1$), the composite particle ceases to be an elementary scatterer because now it is impossible to travel from point 1 to point 2 inside the composite particle without going through vacuum. Thus, criterion 1 suggests that composite particles with inclusions in the form of vacuum voids cannot be considered elementary scatterers. It is obvious, however, that the composite particle with $m_2 \neq 1$ is no more an elementary scatterer than the same particle but with $m_2 = 1$.

To demonstrate the irrelevance of the second criterion, let us consider a composite particle shown in Fig. 18(b) and consisting of four nested parts with refractive indices m_1, m_2, m_3, and m_4, respectively. If none of the refractive indices is equal to 1, then the second criterion suggests that this particle is an elementary scatterer. Indeed, breaking this particle into two parts as shown in Fig. 18(c) changes the refractive indices of the parts relative to their immediate surroundings: the refractive index of the interior of the left component changes from m_3 to 1, and the refractive index of the exterior of the right component changes from m_2 to 1. However, the composite particle ceases to be an elementary scatterer if $m_2 = m_3 = 1$. Indeed, in this case the partitioning of the composed particle as shown in Fig. 18(c) does not change the refractive indices of the components relative to their immediate surroundings. Again, it is clear that the composite particle with $m_2 \neq 1$ and $m_3 \neq 1$ is no more an elementary scatterer than the same particle but with $m_2 = m_3 = 1$.

The aim of the two criteria of Paper 2 is obvious: to artificially oppose an interface separating vacuum and a material medium to an interface separating two material media. Thus, instead of analyzing what makes different a large isolated particle from the same particle as part of a densely packed medium (Figs. 15 and 16), Paper 2 claims that an interface separating vacuum and a material medium is *qualitatively* different from an interface separating two different material media. However, there is no *qualitative* difference between these two types of interfaces since both of them result in light scattering. Even *quantitatively*, an interface separating vacuum and a medium with refractive index m is identical to an interface between two media with refractive indices m_1 and $m_2 = mm_1$, respectively. As our discussion above and Fig. 15 show, widely separated large composite particles are elementary scatterers whatever their morphology is and regardless of whether or not their morphology obeys the two artificial criteria of Paper 2. However, the same particles cease to be elementary scatterers when they become densely packed.

Paper 2 describes an experiment which is supposed to provide an ultimate proof of Hapke's assumptions. Figure 4 of Paper 2 shows experimentally measured bidirectional reflectances of two different particulate media. The first one was composed of elementary mineral grains with sizes 74 to 105 μm, while the second one was composed of coarse basalt particles consisting of the elementary grains welded together and having sizes 1000 to 1325 μm. Paper 2 claims that

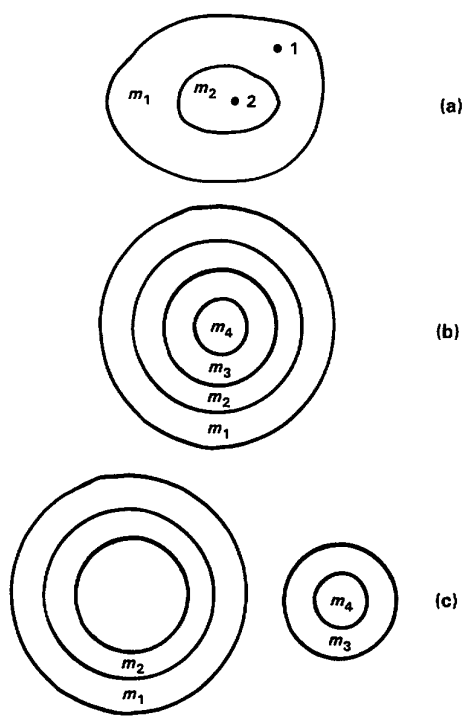

Fig. 18. Demonstration of the irrelevance of the definition of elementary composite scatterers from Paper 2 (see text).

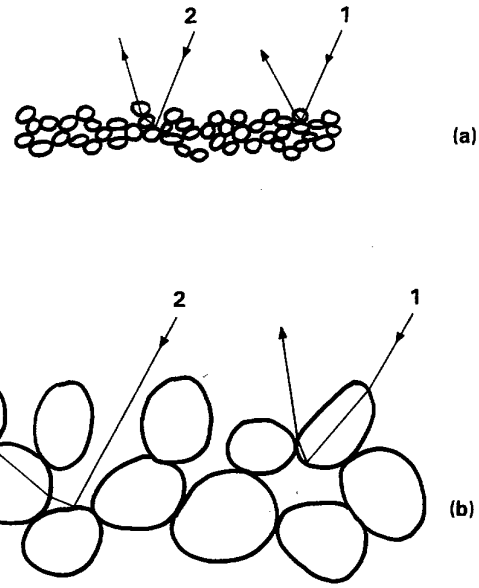

Fig. 19. On the explanation of bidirectional reflectance differences between coarse and fine particle surfaces (see text).

bidirectional reflectance differences between the two samples provide an unequivocal proof of the following two hypotheses: (1) the single, elementary scatterers in a medium consisting of large, composite, densely packed particles are the composite particles themselves, and (2) natural composite particles are backscattering. Paper 2 is correct in that laboratory experiments are an important contributor to the development of science. However, an experiment is often meaningless if it is not a true controlled laboratory measurement† and is not accompanied by physically based theoretical computations. What is shown in Fig. 4 of Paper 2 is an indirect laboratory observation rather than a true controlled laboratory measurement. First of all, the individual particle phase functions have not been measured directly. Second, no complete physical specification of the samples has been provided, which makes impossible a comparison of the measurements with physically based theoretical computations in order to retrieve the phase functions indirectly. Therefore, Fig. 4 of Paper 2 provides anything but the unequivocal proof of the two hypotheses. The most obvious difference between the two measured samples is that the coarse powder is darker. However, this comes at no surprise, as Fig. 19 illustrates. Indeed, a photon entering a 10 times bigger absorbing particle has to travel a much longer path before it exits the particle and, therefore, has a much greater probability to be absorbed [compare photon 1 in Fig. 19(a) and photon 1 in Fig. 19(b)]. Furthermore, the morphology of the boundary layer is dramatically different for a sample composed of 74–105 μm particles from that for a sample composed of particles that are 10 times larger. In particular, a photon incident on the coarse particle sample has a larger probability to penetrate very deeply into the medium without scattering [photon 2 in Fig. 19(b)]. To exit the medium, this photon has to travel a long path inside large absorbing particles and has a greater probability to be absorbed [compare photon 2 in Fig. 19(a) and photon 2 in Fig. 19(b)]. This boundary effect is expected to be especially pronounced at larger phase angles, and this is exactly what Fig. 4 of Paper 2 demonstrates. Thus, Fig. 4 of Paper 2 can be qualitatively explained without assuming that the densely packed large particles are elementary scatterers and/or are backscattering. Another factor that can contribute to the reflectance differences between the two samples is surface roughness on the scale of several particle diameters. Again, this effect is expected to show up at larger phase angles and can explain the measured drop of intensities at phase angles

†The term "controlled laboratory measurement" means that a precise laboratory measurement is accompanied by a complete specification of the measured sample. In our case, this means an accurate specification of particle size and shape distributions, refractive indices, internal structure, compaction state, statistics of particle positions, and microscopic and macroscopic surface roughness.

larger than 120°. It is interesting to note in this regard that the original version of Paper 2 contained a figure that showed quite different reflectances than those in Fig. 4 of Paper 2 even though they were measured for exactly the same samples and at exactly the same scattering geometry. The differences were especially noticeable at large phase angles where the original reflectivities exhibited a pronounced increase rather than a decrease. An obvious explanation of these differences is that the measurements shown in Fig. 4 of Paper 2 pertain to the same samples but with rougher surfaces than those originally measured. This also demonstrates that it is quite easy to conclude that the particle phase function lacks a forward-scattering component if one ignores the fact that this component can be masked by microscopic surface roughness.

5. SUMMARY AND CONCLUSIONS

Paper 1 has pointed out that when the phenomenological Hapke model of bidirectional reflectance by particulate media is used to analyze experimental data for laboratory samples and terrestrial and planetary surfaces, it often yields negative values of the asymmetry parameter of the single-scattering phase function. Since homogeneous dielectric particles with sizes larger than the wavelength have positive asymmetry parameters even when they are densely packed (Paper 1), Paper 2 hypothesizes that the negative asymmetry parameters retrieved with the model are caused by a complicated internal structure of planetary regolith particles. In this paper, we have tested this hypothesis by using state-of-the-art theoretical techniques to compute asymmetry parameters for large isolated and densely packed particles with multiple internal inclusions and size typical of planetary regolith grains. Our computations show that it is essentially impossible to make asymmetry parameters of regolith particles negative by filling the particles with large numbers of internal inclusions. Furthermore, the hypothesis that the negative asymmetry parameters retrieved with the phenomenological model are real and are caused by a complicated internal structure of regolith particles contradicts the results of laboratory phase function measurements for large heterogeneous particles of terrestrial and interplanetary origin[43] and remote-sensing phase function retrievals for interplanetary dust particles.[44] Moreover, the model has retrieved negative asymmetry parameters even for transparent glass particles with no internal scatterers,[47] which is physically meaningless.

The results of Paper 1 strongly suggest that in many cases the retrieved negative asymmetry parameters are likely to be numerical artefacts resulting from the approximations made in the phenomenological approach and its intrinsic inability to reject unphysical solutions. Retrieving the asymmetry parameter from measurements of bidirectional reflectance is an ill-posed inverse problem. Since the range of scattering angles covered by measurements is often strongly restricted, and because the effect of the forward-scattering component of the phase function on reflectance at large phase angles can be neutralized by microscopic surface roughness, physically based constraints are necessary to reject wrong solutions. Unfortunately, the Hapke model does not provide such constraints and, because of its phenomenological nature, cannot even be tested against results of controlled laboratory experiments. As a consequence, applications of the model to laboratory measurements and terrestrial and planetary observations have already led to physically meaningless or suspicious conclusions. Furthermore, we have shown that the model inherently violates the energy conservation law and can grossly disagree with exact solutions of the radiative transfer equation.

The process of multiple light scattering by surfaces consisting of densely packed particles is physically much more complicated than the process of multiple light scattering by sparsely distributed cloud particles. Yet calculations of cloud bidirectional reflectance are always based on numerically accurate solutions of the radiative transfer equation rather than on oversimplified approximations like the Hapke model. It is hard to imagine that the extremely complicated bidirectional reflectance of heterogeneous surfaces can be physically correctly described by a simplistic phenomenological model, the only dubious advantage of which is that it can be implemented on a hand calculator rather than on a workstation or a PC. Instead, advanced modeling of the bidirectional reflectance should at least be based on physically correct single-scattering calculations and numerically accurate solutions of the radiative transfer equation. The next step in the order of increasing model complexity and adequacy is to take into account

the effects of microscopic and macroscopic surface roughness and, ultimately, the discontinuous and stochastic nature of light scattering by planetary surfaces.

Acknowledgements—We are grateful to L. D. Travis, K. Lumme, J. W. Hovenier, A. A. Lacis, J. Haferman, and an anonymous referee for useful comments on a preliminary version of this paper and to E. Ravin and N. T. Zakharova for programming support and help with graphics. The first author thanks B. Hapke for sending proofs of Paper 2 prior to publication. This work was supported in part by the NASA FIRE III program and by the NASA Goddard Institute for Space Studies Planetary Program.

REFERENCES

1. Hansen, J. E. and Travis, L. D., *Space Sci. Rev.*, 1974, **16,** 527.
2. Goody, R. M. and Yung, Y. L., *Atmospheric Radiation*, Oxford University Press, 1989.
3. Stephens, G. L., Tsay, S.-I., Stackhouse, P. W. and Flatau, P. J., *J. Atmos. Sci.*, 1990, **47,** 1742.
4. Lacis, A., Hansen, J. and Sato, M., *Geophys. Res. Lett.*, 1992, **19,** 1607.
5. Brown, R. H. and Matson, D. L., *Icarus*, 1987, **72,** 84.
6. Matson, D. L. and Brown, R. H., *Icarus*, 1989, **77,** 67.
7. Fanale, F. P., Salvail, J. R., Matson, D. L. and Brown, R. H., *Icarus*, 1990, **88,** 193.
8. Mishchenko, M. I., *JQSRT*, 1994, **52,** 95.
9. Balescu, R., *Equilibrium and Nonequilibrium Statistical Mechanics*, Wiley, New York, NY, 1975.
10. Twersky, V., *JOSA*, 1983, **73,** 313.
11. Tsang, L., Kong, J. A. and Shin, R. T., *Radio Sci.*, 1983, **18,** 1260.
12. Hapke, B., *J. Geophys. Res.*, 1981, **86,** 3039.
13. Wolf, P. E., Maret, G., Akkermans, E. and Maynard, R., *J. Phys. (Paris)*, 1988, **49,** 63.
14. Fraden, S. and Maret, G., *Phys. Rev. Lett.*, 1990, **65,** 512.
15. Saulnier, P. M., Zinkin, M. P. and Watson, G. H., *Phys. Rev. B*, 1990, **42,** 2621.
16. Göbel, G., Kuhn, J. and Fricke, J., *Waves Random Media*, 1995, **5,** 413.
17. Muinonen, K., Ph.D. thesis, University of Helsinki, 1990.
18. Muinonen, K., in *Asteroids, Comets, Meteors* 1993, A. Milani et al, eds., p. 271, Kluwer, Dordrecht, 1994.
19. Peltoniemi, J. I., Ph.D. thesis, University of Helsinki, 1993.
20. Hapke, B. *Theory of Reflectance and Emittance Spectroscopy*, Cambridge University Press, New York, NY, 1993.
21. Pinty, B., Verstratete, M. M. and Dickinson, R. E., *Remote Sens. Environ.*, 1989, **27,** 273.
22. Helfenstein, P. and Veverka, J., in *Asteroids II*, R. P. Binzel, T. Gehrels, and M. S. Matthews, eds., p. 557, University of Arizona Press, Tucson, 1989.
23. Bowell, E., Hapke, B., Domingue, D., Lumme, K., Peltoniemi, J. and Harris, A., in *Asteroids II*, R. P. Binzel, T. Gehrels, and M. S. Matthews, eds., p. 524, University of Arizona Press, Tucson, 1989.
24. Hapke, B., *JQSRT*, 1996, **55,** 837.
25. Mishchenko, M. I., Travis, L. D. and Mackowski, D. W., *JQSRT*, 1996, **55,** 535.
26. Wielaard, D. J., Mishchenko, M. I., Macke, A. and Carlson, B. E., *Appl. Opt.* (in press).
27. Muinonen, K., Lumme, K., Peltoniemi, J. and Irvine, W. M., *Appl. Opt.*, 1989, **28,** 3051.
28. Muinonen, K., Nousiainen, T., Fast, P., Lumme, K. and Peltoniemi, J. I., *JQSRT*, 1996, **55,** 577.
29. Macke, A., Mueller, J. and Raschke, E., *J. Atmos. Sci.*, 1996, **53,** 2813.
30. Macke, A., Mishchenko, M. I., Muinonen, K. and Carlson, B. E., *Opt. Lett.*, 1995, **20,** 1934.
31. Borghese, F., Denti, P., Saija, R. and Sindoni, O. I., *JOSA A*, 1992, **9,** 1327.
32. Borghese, F., Denti, P. and Saija, R., *Appl. Opt.*, 1994, **33,** 484; errata, 1995, **34,** 5556.
33. Fuller, K. A., *JOSA A*, 1995, **12,** 893.
34. Videen, G., Ngo, D., Chýlek, P. and Pinnick, R. G., *JOSA A*, 1995, **12,** 922.
35. Mackowski, D. W. and Jones, P. D., *J. Thermophys. Heat Transfer*, 1995, **9,** 193.
36. Lumme, K. and Rahola, J., *Astrophys. J.*, 1994, **425,** 653.
37. Macke, A., Mishchenko, M. I. and Cairns, B., *J. Geophys. Res.*, 1996, **101,** 23311.
38. Macke, A., Mishchenko, M. I. and Cairns, B., in *IRS'96: Current Problems in Atmospheric Radiation*, W. L. Smith and K. Stamnes, eds., Deepack Publ., Hampton, VA (in press).
39. McKay, D., Fruland, R. and Heiken, G., in *Proc. 5th Lunar Science Conf.*, W. Gose, ed., p. 887, Pergamon Press, New York, NY, 1974.
40. Graf, J. C., NASA Ref. Publ. 1265, NASA/JSC, Houston, TX, 1993.
41. van de Hulst, H. C., *Light Scattering by Small Particles*, Wiley, New York, NY, 1957.
42. McGuire, A. F. and Hapke, B. W., *Icarus*, 1995, **113,** 134.
43. Weiss-Wrana, K., *Astron. Astrophys.*, 1983, **126,** 240.
44. Lamy, P. L. and Perrin, J.-M., *Astron. Astrophys.*, 1986, **163,** 269.
45. Hansen, J. E., *J. Atmos. Sci.*, 1969, **26,** 478.
46. Hansen, J. E. and Pollack, J. B., *J. Atmos. Sci.*, 1970, **27,** 265.
47. Hapke, B. and Wells, E., *J. Geophys. Res.*, 1981, **86,** 3055.
48. Verbischer, A. J. and Veverka, J., *Icarus*, 1990, **88,** 418.
49. Hapke, B., *J. Atmos. Sci.*, 1976, **33,** 1803.
50. Hansen, J. E. and Hovenier, J. W., *J. Atmos. Sci.*, 1974, **31,** 1137.

51. Helfenstein, P., Veverka, J. and Hillier, J., *Icarus* (in press).
52. Russel, E. E., Brown, F. G., Chandos, R. A., Fincher, W. C., Kubel, L. F., Lacis, A. A. and Travis, L. D., *Space Sci. Rev.*, 1992, **60,** 531.
53. Deschamps, P.-Y., Bréon, F.-M., Leroy, M., Podaire, A., Bricaud, A., Buriez, J.-C. and Séze, G., *IEEE Trans. Geosci. Remote Sens.*, 1994, **32,** 598.
54. King, M. D., Kaufman, Y. J., Menzel, W. P. and Tanré, D., *IEEE Trans. Geosci. Remote Sens.*, 1992, **30,** 2.
55. Diner, D. J., Bruegge, C. J., Martonchik, J. V., Bothwell, G. W., Danielson, E. D., Floyd, E. L., Ford, V. G., Hovland, L. E., Jones, K. L. and White, M. L., *Int. J. Imaging Syst. Technol.*, 1991, **3,** 92.
56. Travis, L. D., *Proc. SPIE*, 1992, **1747,** 154.
57. Hapke, B., *Geophys. Res. Lett.*, 1978, **5,** 1067.
58. Hovenier, J. W., *Astron. Astrophys.*, 1970, **7,** 86.
59. van de Hulst, H. C., *Multiple Light Scattering*, Academic Press, New York, NY, 1980.
60. Chandrasekhar, S., *Radiative Transfer*, Dover, New York, NY, 1960.
61. Goguen, J., submitted to *Icarus*.
62. Jones, P. D., McLeod, D. G. and Dorai-Raj, D. E., *ASME J. Heat Transfer*, 1996, **118,** 94.
63. Ulaby, F. T., Moore, R. K. and Fung, A. K., *Microwave Remote Sensing*, Vols. 1–3, Addison-Wesley, Reading, MA, 1981.
64. Tsang, L., Kong, J. A. and Shin, R. T., *Theory of Microwave Remote Sensing*, Wiley, New York, NY, 1985.
65. Fung, A. K., *Microwave Scattering and Emission Models and Their Applications*, Artech House, Boston, MA, 1994.
66. Stephens, G. L., *Remote Sensing of the Lower Atmosphere*, Oxford University Press, New York, NY, 1994.
67. Kawabata, K., Coffeen, D. L., Hansen, J. E., Lane, W. A., Sato, M. and Travis, L. D., *J. Geophys. Res.*, 1980, **85,** 8129.
68. Sato, M. and Travis, L. D., *Icarus*, 1996, **124,** 569.
69. Mishchenko, M. I. and Travis, L. D., *J. Geophys. Res.* (in press).
70. Dlugach, J. M. and Yanovitskij, E. G., *Icarus*, 1974, **22,** 66.
71. de Haan, J. F., Bosma, P. B. and Hovenier, J. W., *Astron. Astrophys.*, 1987, **183,** 371.
72. Stamnes, K., Tsay, S-C., Wiscombe, W. and Jayaweera, K., *Appl. Opt.*, 1988, **27,** 2502.
73. de Rooij, W. A., Ph.D. thesis, Free University, Amsterdam, 1985.
74. Mishchenko, M. I., *JQSRT*, 1991, **46,** 171.
75. Stephens, G. L., *J. Atmos. Sci.*, 1988, **45,** 1818.
76. Lumme, K., Peltoniemi, J. I. and Irvine, W. M., *Transport Theory Statist. Phys.*, 1990, **19,** 317.
77. Barker, H. W. and Davies, J. A., *J. Atmos. Sci.*, 1992, **49,** 1115.
78. Peltoniemi, J. I., *JQSRT*, 1993, **50,** 655.
79. Cahalan, R. F., Ridgway, W., Wiscombe, W. J., Bell, T. L. and Snider, J. B., *J. Atmos. Sci.*, 1994, **51,** 2434.
80. Myneni, R. B., Marshak, A. L. and Knyazikhin, Y. V., *JQSRT*, 1991, **46,** 259.
81. Tien, C. L., *ASME J. Heat Transfer*, 1988, **110,** 1230.
82. Tien, C.-L. and Vafai, K., *Adv. Appl. Mech.*, 1990, **27,** 225.
83. Peltoniemi, J. I. and Lumme, K., *JOSA A*, 1992, **9,** 1320.
84. Yang, Y. S., Howell, J. R. and Klein, D. E., *ASME J. Heat Transfer*, 1983, **105,** 325.
85. Argento, C. and Bouvard, D., *Int. J. Heat Mass Transfer*, 1996, **39,** 3175.
86. Keller, J. B., *JOSA*, 1962, **52,** 116.